NASA TECHNICAL NOTE

NASA TN D-2243

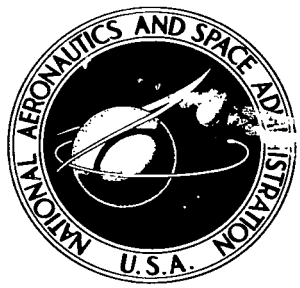

NASA TN D-2243

EFFECTS OF AIRCRAFT RELATIVE DENSITY ON SPIN AND RECOVERY CHARACTERISTICS OF SOME CURRENT CONFIGURATIONS

by William D. Grantham and Sue B. Grafton

Langley Research Center
Langley Station, Hampton, Va.

NATIONAL AERONAUTICS AND SPACE ADMINISTRATION • WASHINGTON, D. C. • MARCH 1965

NASA TN D-2243

EFFECTS OF AIRCRAFT RELATIVE DENSITY ON SPIN AND RECOVERY CHARACTERISTICS OF SOME CURRENT CONFIGURATIONS

By William D. Grantham and Sue B. Grafton

Langley Research Center
Langley Station, Hampton, Va.

NATIONAL AERONAUTICS AND SPACE ADMINISTRATION

For sale by the Office of Technical Services, Department of Commerce,
Washington, D.C. 20230 -- Price $2.00

EFFECTS OF AIRCRAFT RELATIVE DENSITY ON SPIN AND RECOVERY CHARACTERISTICS OF SOME CURRENT CONFIGURATIONS

By William D. Grantham and Sue B. Grafton
Langley Research Center

SUMMARY

An analytical study has been conducted on a high-speed digital computer utilizing six-degree-of-freedom equations of motion to examine the effects of relative density on the spin and recovery characteristics of four configurations which are representative of modern airplanes. Two approaches were used: Computations were made simulating conditions for which the airplane obtained a disturbance that put it at a high angle of attack with applied rotation in a near-developed spin condition at various initial altitudes to determine whether a developed spin would ensue. After it was determined that developed spins did ensue in the first group of calculations, separate calculations were made to determine whether a spin could be entered starting at or near trimmed gliding flight (1 g stall maneuvers).

The results indicate that the effects of changing relative density on developed spins and recoveries were as follows: An increase in relative density gave faster rotating spins, higher rates of descent, lower values of the spin coefficient, little change in angles of attack and sideslip, and recoveries, if obtained, were slower. Changes in relative density can make the difference between a spin and a no-spin when entry is attempted by means of a 1 g stall maneuver, but the effect of relative density is not consistent. About the only generalization that can be made on the effect of relative density on the spin entry is that increases in relative density cause increased roll oscillations during the spin-entry motions.

INTRODUCTION

Reference 1 describes the results of model tests made more than 20 years ago in the Langley 20-foot free-spinning tunnel to determine the effects of relative density on spin and recovery characteristics of airplanes. In that study, the range of relative-density parameters used was 6 to 12. Over the ensuing years, airplane configurations have changed considerably and the range of values of relative density has greatly increased. An analytical study has, therefore, been made to examine the effects of relative density on spinning for

four more recent configurations, and the results are reported herein. In this study the range of relative-density parameters covered was from 17 to 487. The present paper also includes consideration of spin-entry characteristics, whereas reference 1 was concerned only with fully developed spins and recoveries therefrom.

The four configurations used in this study were considered to be representative of modern aircraft and were as follows: a stub-wing research vehicle, a sweptback wing fighter, a delta-wing bomber, and a delta-wing fighter. The relative-density parameter was considered to be varied by changing altitude. Included in the study were brief calculations to determine the effect of varying the magnitude of some of the aerodynamic parameters for various simulated altitudes.

SYMBOLS

The body system of axes is used. This system of axes, related angles, and positive directions of corresponding forces and moments are illustrated in figure 1.

b wing span, ft

C_l rolling-moment coefficient, $\frac{M_X}{\frac{1}{2}\rho V_R^2 Sb}$

C_m pitching-moment coefficient, $\frac{M_Y}{\frac{1}{2}\rho V_R^2 S\bar{c}}$

C_n yawing-moment coefficient, $\frac{M_Z}{\frac{1}{2}\rho V_R^2 Sb}$

C_X longitudinal-force coefficient, $\frac{F_X}{\frac{1}{2}\rho V_R^2 S}$

C_Y side-force coefficient, $\frac{F_Y}{\frac{1}{2}\rho V_R^2 S}$

C_Z vertical-force coefficient, $\frac{F_Z}{\frac{1}{2}\rho V_R^2 S}$

$\bar{c}$ mean aerodynamic chord, ft

F_X longitudinal force acting along X body axis, lb

F_Y side force acting along Y body axis, lb

F_Z vertical force acting along Z body axis, lb

g acceleration due to gravity, ft/sec^2

g_o acceleration due to gravity at sea level, 32.17 ft/sec^2

h_0 altitude at beginning of time increment, ft

h_1 altitude at end of time increment, ft

I_X, I_Y, I_Z moments of inertia about X, Y, and Z body axes, respectively, slug-ft^2

M_X rolling moment acting about X body axis, ft-lb

M_Y pitching moment acting about Y body axis, ft-lb

M_Z yawing moment acting about Z body axis, ft-lb

m mass of airplane, W/g, slugs

p, q, r components of resultant angular velocity about X, Y, and Z body axes, respectively, radians/sec

R radius of earth, 3,956.67 miles

S wing-surface area, sq ft

t time, sec

u, v, w components of resultant velocity V_R along X, Y, and Z body axes, respectively, ft/sec

V vertical component of velocity of airplane center of gravity (rate of descent), ft/sec

V_R resultant linear velocity, ft/sec

W weight, lb

X,Y,Z longitudinal, lateral, and vertical body axes of airplane, respectively

α angle of attack, angle between relative wind V_R projected into XZ-plane of symmetry and X body axis, positive when relative wind comes from below XY body plane, deg

β angle of sideslip, angle between relative wind V_R and projection of relative wind on XZ-plane, positive when relative wind comes from right of plane of symmetry, deg

δ_a total deflection of left and right ailerons with respect to each other, positive with trailing edge of right aileron down (left stick), deg

δ_e elevator deflection with respect to fuselage reference line, positive with trailing edge down, deg

δ_r rudder deflection with respect to fin, positive with trailing edge to left, deg

θ_e total angular movement of X body axis from horizontal plane measured in vertical plane, positive when airplane nose is above horizontal plane, deg

μ airplane relative-density parameter, $\frac{W}{g\rho Sb}$

ρ air density, slugs/cu ft

Ω resultant angular velocity, radians/sec

ϕ angle between Y body axis and horizontal measured in vertical plane, positive for erect spins when right wing is downward and for inverted spins when left wing is downward, deg

ϕ_e total angular movement of Y body axis from horizontal plane measured in YZ body plane, positive when clockwise as viewed from rear of airplane (if X body axis is vertical, ϕ_e is measured from a reference position in horizontal plane), deg

ψ_e horizontal component of total angular deflection of X body axis from reference position in horizontal plane, positive when clockwise as viewed from vertically above airplane, deg

$C_{l_{\delta_a}}$ incremental rolling-moment coefficient due to aileron deflection, per deg

$C_{l_{\delta_r}}$ incremental rolling-moment coefficient due to rudder deflection, per deg

$C_{n_{\delta_a}}$ incremental yawing-moment coefficient due to aileron deflection, per deg

$C_{n_{\delta_r}}$ incremental yawing-moment coefficient due to rudder deflection, per deg

$C_{Y_{\delta_a}}$ incremental side-force coefficient due to aileron deflection, per deg

$C_{Y_{\delta_r}}$ incremental side-force coefficient due to rudder deflection, per deg

$$C_{l_p} = \frac{\partial C_l}{\partial\left(\frac{pb}{2V_R}\right)} \qquad C_{n_\beta} = \frac{\partial C_n}{\partial \beta}$$

$$C_{l_r} = \frac{\partial C_l}{\partial\left(\frac{rb}{2V_R}\right)} \qquad C_{Y_\beta} = \frac{\partial C_Y}{\partial \beta}$$

$$C_{l_{\dot{\beta}}} = \frac{\partial C_l}{\partial\left(\frac{\dot{\beta}b}{2V_R}\right)} \qquad C_{n_p} = \frac{\partial C_n}{\partial\left(\frac{pb}{2V_R}\right)}$$

$$C_{m_q} = \frac{\partial C_m}{\partial\left(\frac{q\bar{c}}{2V_R}\right)} \qquad C_{n_r} = \frac{\partial C_n}{\partial\left(\frac{rb}{2V_R}\right)}$$

$$C_{l_\beta} = \frac{\partial C_l}{\partial \beta} \qquad C_{n_{\dot{\beta}}} = \frac{\partial C_n}{\partial\left(\frac{\dot{\beta}b}{2V_R}\right)}$$

A dot over a symbol represents a derivative with respect to time.

PROCEDURES AND CALCULATIONS

Spin entry and developed spin motions were calculated by a high-speed digital computer which solved the equations of motion and associated formulas listed in the appendix. The equations of motion are Euler's equations representing six degrees of freedom along and about the airplane body system of axes. (See fig. 1 for illustration of body axes.) The mass and dimensional characteristics used in the calculations are listed in table I and the planviews of the four configurations designated A, B, C, and D are shown in figure 2.

In general, the aerodynamic data used were nonlinear as shown in figures 3 to 8. The data for these plots were obtained from references 2 to 7. No measured values of the lateral force increments resulting from deflecting the ailerons and rudder were available for configuration B. (See figs. 5 and 6.) Inasmuch as previous studies have indicated that these incremental forces have little or no effect on spin entry and spin characteristics no attempt was made to estimate them.

The oscillation-type rotary derivatives presented in figures 7 and 8 were obtained as combination derivatives which include the effects of $\dot{\beta}$ - that is, C_{l_p} is actually $\left(C_{l_p} + C_{l_{\dot{\beta}}} \sin \alpha\right)$, C_{n_p} is actually $\left(C_{n_p} + C_{n_{\dot{\beta}}} \sin \alpha\right)$, C_{l_r} is actually $\left(C_{l_r} - C_{l_{\dot{\beta}}} \cos \alpha\right)$, C_{n_r} is actually $\left(C_{n_r} - C_{n_{\dot{\beta}}} \cos \alpha\right)$, and so forth. However, inasmuch as the full derivatives could not be separated into their component parts, it was arbitrarily decided for this study to treat the derivatives as though they were due solely to angular velocities about body axes. The rolling moment due to yawing C_{l_r} and the yawing moment due to rolling C_{n_p} parameters were set equal to zero for configurations A and B. For all configurations, no effects of rolling and yawing on side force were included. In addition, constant values of C_{m_q} were used for each configuration as follows: Configuration A, $C_{m_q} = -10$; configurations B and C, $C_{m_q} = -2$; and configuration D, $C_{m_q} = -1$.

Two approaches were used: Computations were made simulating conditions for which the airplane obtained a disturbance that put it at a high angle of attack with applied rotation in a near-developed spin condition at each altitude (that is h_0 = 15,000 feet, 30,000 feet, 45,000 feet, and 60,000 feet) to determine whether a developed spin would ensue. This technique simulated that used in the Langley 20-foot free-spinning tunnel in which small dynamic models are launched in near-developed spin conditions and then freely proceed to either developed spins or to "no-spin" dive-out or roll-over motions, depending upon the design and mass characteristics. After it was determined that developed spins did ensue in the first group of calculations, separate calculations were made to determine whether a spin could be entered starting at or near trimmed gliding flight (1 g stall maneuver).

Spin recovery attempts were made by deflecting the rudder against the direction of yaw and the ailerons with the direction of yaw (left rudder and right stick when spinning to the pilot's right), because these control deflections are the optimum for recovery from developed spins for airplanes loaded heavily along the fuselage (see ref. 8), as are the subject configurations. The elevators were left in the initial up position for all cases. During the present study, a spin is considered to be terminated when either the spin-rotation ceases or the angle of attack becomes and remains less than the stall angle within 10 turns after the recovery controls are applied. Usually when the angle of attack becomes less than the stall angle, the airplane enters a steep dive without significant rotation ($r \approx 0$). In some cases, however, the airplane may be turning or rolling in a spiral glide or an aileron roll. Also, sometimes the airplane may roll or pitch to an inverted attitude from the erect spin and may still have some rotation, but it is out of the original erect spin.

RESULTS AND DISCUSSION

The calculated results are presented in figures 9 to 16 as time histories of angle of attack α, angle of pitch θ_e, angle of sideslip β, angle of roll ϕ_e, yawing velocity r, control-surface positions, and spin turns completed. It should be noted that the scales on these figures are not consistent and the reader should be careful when trying to compare various time histories. Also, it may be noted that attempted recoveries are indicated by dashed lines, spins by solid lines.

Simulated Launching With Rotary Motion

Elevator up, rudder right, and stick left conditions were used in each calculation to promote a spin to the pilot's right. The initial flight conditions used at each relative density investigated are presented in table II.

The calculated results for all configurations showed that developed spins ensued from launchings at all four altitudes; the magnitudes of the pertinent parameters are presented in table III.

Configuration A.- Two representative time histories for configuration A are presented as figure 9. Figure 9(a) represents the motion obtained starting at 15,000 feet ($\mu = 73$) and indicates that after approximately 10 turns a developed spin condition had been achieved. The angle of attack was oscillating from approximately 84° to 89°, the angle of sideslip was oscillating from 1° to -8°, and the rate of yaw was approximately 2.8 radians per second. This is the point at which the recovery attempt was made, and as seen in figure 9(a) no recovery was achieved within 10 additional turns. Figure 9(b) represents the spin obtained by starting at 60,000 feet ($\mu = 487$) and shows that after approximately 10 turns $\alpha \approx 85^\circ$ to 88°, $\beta \approx 0^\circ$ to -4°, and $r \approx 3.1$ radians per second. A recovery was attempted at that point and, as shown, none was achieved within 10 additional turns.

The results obtained for this configuration indicate that an increase in the relative density gave slightly faster rotating spins, higher rates of descent, and lower values of the spin coefficient $\Omega b/2V_R$. The small changes in angle of attack and sideslip are negligible.

Configuration B.- Two representative time histories of the spin and recovery motions obtained for configuration B are presented as figure 10.

Pertinent results from these calculations indicate that when this configuration was launched into a near-spin condition, an increase in the relative density gave faster rotating spins, higher rates of descent, lower values of the spin coefficient, and slower recoveries. The effect of relative density variations on the angles of attack and sideslip experienced during these four spins was again considered to be negligible. (See table III.)

Configuration C.- Spins were obtained at all four altitudes for configuration C, from which no recoveries were achieved. Two representative time histories are presented as figure 11.

The results (table III) indicate that, as in the case of configurations A and B already discussed, when this configuration was launched into a near-spin condition, an increase in the relative density gave slightly faster rotating spins, higher rates of descent, and lower values of the spin coefficient; however, there was little change in the angles of attack and sideslip.

Configuration D.- The calculated time histories for configuration D show that recoveries were achieved from each spin. Two representative time histories of the spin and recovery are presented as figure 12.

The results shown in table III indicate that, as in the case of the configurations already discussed, when this configuration was launched into a near-spin condition, an increase in the relative density gave faster rotating spins, higher rates of descent, lower values of the spin coefficient, and slower recoveries. The small changes in angles of attack and sideslip were again considered to be negligible.

Summation of results for launchings with rotary motion.- It was concluded from the results discussed thus far that developed spins ensued for all configurations and initial conditions studied, and that the effects of variations in relative density were similar on all of the configurations; that is, an increase in relative density gave faster rotating spins, higher rates of descent, lower values of the spin coefficient, little change in angle of attack and sideslip, and recoveries, if obtained, were slower. These results are considered to be in general agreement with those of reference 1; except that in the former study, somewhat larger effects of relative density on angle of attack and sideslip appeared to be indicated.

Simulated Spin Entry Motion

After it was found that, once achieved, developed spins could be maintained for all cases investigated, attempts were made for each configuration to enter the spin starting at or near trimmed gliding flight and flying the airplane up through the stall angle of attack (1 g stall maneuver). Back stick was used to stall the craft, right rudder was applied at or just after the stall to yaw the craft to the right, and left stick was applied variously timed, to attempt to promote spin entries to the right in all calculations. Calculations were made that simulated initial altitudes of 15,000, 30,000, 45,000 and 60,000 feet for each of the four configurations, as was done for the computations where each craft was launched with applied rotation. Initial conditions used are shown in the second part of table II.

Configuration A.- The calculated time histories for configuration A are presented as figure 13, and, as can be seen, spins were obtained at all four altitudes.

Ccmparison of the spins at four altitudes (fig. 13) indicates that the only noticeable effect of change in relative density on the spin entry characteristics is that as the relative density is increased the roll angles experienced during the initial phases of the spin entry are larger and that the ensuing rolling and pitching motions were more oscillatory. After approximately five spinning turns, the spin motions achieved at the various altitudes are similar.

Recoveries were attempted from each of these spins after seven spinning turns had been completed from initial 1g stall entry and, as can be seen from the respective time histories, it took approximately 6 to 7 additional turns to achieve recovery in each instance. It is believed that the reason recoveries, even though poor, were possible from these spins whereas, as previously discussed, they were not obtained from the spins which ensued after this configuration was launched in a near-spin condition is that in the second group of calculations, the recovery controls were applied before the spin-rotation rates had increased to the magnitudes experienced in the first group of calculations. The lower rotation rates enabled recoveries, even though poor, to be achieved.

Configuration B.: The computed time histories for configuration B are presented in figure 14. The characteristics of motions obtained in the attempted spin entries were very different for the different altitudes, but there was no consistent trend in the results. For example, when a spin entry was attempted at an altitude of 15,000 feet (fig. 14(a)), the craft rolled over to the right ($\phi_e > 360^\circ$) and then continued to oscillate in roll to such an extent that no spin was obtained; whereas, for an initial altitude of 30,000 feet (fig. 14(b)), the craft rolled over to the right, maintained an angle of attack above the stall angle, began to oscillate approximately $\pm 15^\circ$ in roll, and continued to spin. The time history shown in figure 14(c), which was computed by using an initial altitude of 45,000 feet, shows that the craft rolled over to the right twice ($\phi_e > 700^\circ$) and then continued to roll until such time as the angle of attack became less than zero. The direction of turning was steadily changing and therefore could not be called a spin. When a spin entry was attempted by using an initial altitude of 60,000 feet (fig. 14(d)), the craft rolled over to the right twice and began to oscillate from approximately -50° to 70° in roll angle and made three spinning turns to the right before it oscillated out of the spin. The angle of attack became less than zero and the rate of yaw was approaching zero when the computation was stopped. No recovery was attempted from the only spin obtained (i.e., at $h_0 = 30{,}000$ feet).

Configuration C.- The time histories for configuration C are presented in figure 15 and, as can be seen, spins were entered at each altitude. Again, as in the spins entered with configuration A, the computed rolling and pitching motions were more oscillatory for the higher values of relative density.

Recoveries were attempted from these spins after seven turns had been completed with the following results: (1) no recovery was achieved from the spin at 15,000 feet, (2) recovery was achieved from the spin at 30,000 feet in approximately two additional turns, (3) less than one additional turn was required to achieve recovery from the spin at 45,000 feet. (See figs. 15(a) to 15(c), respectively.) No recovery was attempted from the spin obtained at an initial altitude of 60,000 feet. Apparently, the primary reason that

recoveries were obtained at the higher altitudes and not at 15,000 feet is that at the higher altitudes the spin motions were more oscillatory and the rotation rates slower. This is also the probable reason why no recoveries were achieved from the spin obtained by launching the craft with applied rotation (table III); those spins were more steady in nature and yawing at a somewhat faster rate when recovery controls were applied. (Compare fig. 11 with fig. 15.)

Configuration D.- The calculated time histories for configuration D are presented in figure 16. It is shown that spins were entered at each altitude investigated except at 60,000 feet, wherein the craft rolled to such an extent that a spin entry was prevented. No recoveries were attempted for any condition. About the only generalization that can be made about the results for configuration D is that as the relative density was increased the amount of roll experienced increased.

Summation of results of spin entry calculations.- It is concluded from these calculations that there is no consistent effect of relative density on whether an airplane has more or less tendency to enter a spin. About the only generalization that can be drawn from the results of the spin entry calculations is that increasing relative density causes larger roll-angle oscillations in the initial phases of the spin-entry attempt. Apparently, changes in relative density can affect the roll characteristics to such an extent that spins may or may not be obtained from a 1 g stall maneuver for configurations and conditions, all of which would spin when launched with spinning rotation. For example, for two of the subject configurations, spins could be entered over the complete range of relative density investigated; for the third configuration, spins could be entered at all relative densities except the maximum studied. For the fourth configuration, spins could be entered at a medium value of relative density (craft rolled over to the right once, began to oscillate $\pm 15^{\circ}$ and continued spinning), but when the relative density was appreciably decreased or increased, no spin could be entered (rolling did not stop after initial roll over).

It appears that in order to predict the effect of changing relative density on spin-entry characteristics for any particular configuration, an investigation must be made on the specific design.

AERODYNAMIC VARIATIONS

Inasmuch as it was found that there were some altitudes at which some configurations would not enter a spin by means of a 1 g stall maneuver, and that the roll-motion characteristics were very important in determining whether a spin could be entered, a few calculations were made to determine whether large increases in the values of C_{l_p} and C_{l_β} (arbitrary values used were twice the basic values) would enable spins to be entered at these altitudes.

As mentioned previously, spins on configuration D were entered at all altitudes except the maximum (60,000 feet). Additional calculations were made wherein the basic values of C_{l_p} and C_{l_β} were arbitrarily increased by

various amounts in an attempt to enter a spin at a simulated altitude of 60,000 feet with this configuration. The resulting time histories showed that increasing the negative values of C_{l_p} did not enable a spin to be entered, whereas the larger negative values of C_{l_β} (increased effective dihedral) allowed a spin entry. These effects are in agreement with the results obtained during previous analytical studies of the spin characteristics of other delta wing configurations and indicated that the magnitude of C_{l_p} had little effect on the initial phases of the spin entry, although the magnitude of C_{l_p} can affect the spin after it has developed. Also, as to the effects of C_{l_β} on spin entries, it has been pointed out in references 3 and 9 that the magnitude of C_{l_β} can determine whether an aircraft can enter a spin.

As discussed previously, spins could be entered on configuration B at an altitude of 30,000 feet, but if the altitude was reduced to 15,000 feet or increased to 45,000 and 60,000 feet, no spins could be entered. Some calculations were made wherein the basic values of C_{l_p} and C_{l_β} were arbitrarily increased by various amounts in an attempt to enter spins at 15,000 feet and 60,000 feet. The time histories computed for an initial altitude of 15,000 feet indicated that increasing the basic negative values of C_{l_p} or C_{l_β} still would not enable a spin to be entered. However, when the increased negative values of both C_{l_p} and C_{l_β} were used, the craft did enter a spin. The results at 60,000 feet showed that when larger negative values of C_{l_p} and/or C_{l_β} were used, spins could not be entered.

These results indicate that even when relatively large negative values of C_{l_p} and/or C_{l_β} are used, spins cannot always be entered at any given altitude on all configurations.

CONCLUSIONS

The following conclusions are drawn from the present analytical study on the effects of airplane relative density on spin and recovery characteristics of four configurations representative of modern airplanes.

1. Trends obtained as to the effect of changing relative density on developed spins and recoveries were generally similar to those noted in earlier experimental free-spinning tunnel model tests made for airplanes with unswept wings and a much smaller relative density range, and were as follows: An increase in relative density gave faster rotating spins, higher rates of descent, lower values of the spin coefficient, little change in angle of attack and sideslip, and recoveries, if obtained, were slower.

2. Changes in relative density can make the difference between a spin and a no-spin when entry is attempted by means of a 1 g stall maneuver, but the

effect of relative density is not consistent. About the only generalization that can be made on the effect of relative density on the spin entry is that increases in relative density cause increased roll oscillations during the spin-entry motions.

Langley Research Center,
National Aeronautics and Space Administration,
Langley Station, Hampton, Va., June 3, 1964.

APPENDIX

EQUATIONS OF MOTION AND ASSOCIATED FORMULAS

The equations of motion used in the calculations were:

$$\dot{p} = \frac{I_Y - I_Z}{I_X} qr + \frac{\rho V_R^2 Sb}{2I_X}\left(C_{l_\beta}\beta + C_{l_{\delta_r}}\delta_r + C_{l_{\delta_a}}\delta_a\right) + \frac{\rho V_R Sb^2}{4I_X}\left(C_{l_p}p + C_{l_r}r\right)$$

$$\dot{q} = \frac{I_Z - I_X}{I_Y} pr + \frac{\rho V_R^2 S\bar{c}}{2I_Y} C_m + \frac{\rho V_R S\bar{c}^2}{4I_Y} C_{m_q}q$$

$$\dot{r} = \frac{I_X - I_Y}{I_Z} pq + \frac{\rho V_R^2 Sb}{2I_Z}\left(C_{n_\beta}\beta + C_{n_{\delta_r}}\delta_r + C_{n_{\delta_a}}\delta_a\right) + \frac{\rho V_R Sb^2}{4I_Z}\left(C_{n_p}p + C_{n_r}r\right)$$

$$\dot{u} = -g \sin\theta_e + vr - wq + \frac{\rho V_R^2 S}{2m} C_X$$

$$\dot{v} = g \cos\theta_e \sin\phi_e + wp - ur + \frac{\rho V_R^2 S}{2m}\left(C_{Y_\beta}\beta + C_{Y_{\delta_r}}\delta_r + C_{Y_{\delta_a}}\delta_a\right)$$

$$\dot{w} = g \cos\theta_e \cos\phi_e + uq - vp + \frac{\rho V_R^2 S}{2m} C_Z$$

In addition, the following formulas were used:

$$\alpha = \tan^{-1}\frac{w}{u}$$

$$\beta = \sin^{-1}\frac{v}{V_R}$$

$$V_R = \sqrt{u^2 + v^2 + w^2}$$

$$V = -u \sin\theta_e + v \cos\theta_e \sin\phi_e + w \cos\theta_e \cos\phi_e$$

$$h_1 = h_0 - \Delta t V$$

$$\dot{\theta}_e = q \cos\phi_e - r \sin\phi_e$$

$$\dot{\phi}_e = p + r \tan\theta_e \cos\phi_e + q \tan\theta_e \sin\phi_e$$

$$\dot{\psi}_e = \frac{r \cos \phi_e + q \sin \phi_e}{\cos \theta_e}$$

$$g = g_o \left(\frac{R}{R + \frac{h_1}{5280}} \right)^2$$

$$\text{Turns in spin} = \frac{\int \dot{\psi}_e \, dt}{2\pi}$$

$$\phi_e = \sin^{-1} \frac{\sin \phi}{\cos \theta_e}$$

REFERENCES

1. Seidman, Oscar, and Neihouse, A. I.: Free-Spinning Wind-Tunnel Tests of a Low-Wing Monoplane With Systematic Changes in Wings and Tails. V. Effect of Airplane Relative Density. NACA Rep. 691, 1940.

2. Bowman, James S., Jr., and Grantham, William D.: Low-Speed Aerodynamic Characteristics of a Model of a Hypersonic Research Airplane at Angles of Attack up to 90° for a Range of Reynolds Numbers. NASA TN D-403, 1960.

3. Grantham, William D., and Scher, Stanley H.: Analytical Investigation and Prediction of Spin and Recovery Characteristics of the North American X-15 Airplane. NASA TM X-294, 1960.

4. Hewes, Donald E.: Low-Subsonic Measurements of the Static and Oscillatory Lateral Stability Derivatives of a Sweptback-Wing Airplane Configuration at Angles of Attack From -10° to 90°. NASA MEMO 5-20-59L, 1959.

5. Ammann, Victor R., Jr.: Wind Tunnel Data Report - Low Speed Tests of the 1/40-Scale B-58A High Angle Stability Force Model. Rep. FZT-4-231 (Contract AF 33(600) - 36200), General Dynamics/Fort Worth, Jan. 18, 1961.

6. Paulson, John W.: Low-Speed Measurements of Oscillatory Lateral Stability Derivatives of a Model of a 60° Delta-Wing Bomber. NASA TM X-13, 1959.

7. Scher, Stanley H., Anglin, Ernie L., and Lawrence, George F.: Analytical Investigation of Effect of Spin Entry Technique on Spin and Recovery Characteristics for a 60° Delta-Wing Airplane. NASA TN D-156, 1959.

8. Neihouse, Anshal I., Klinar, Walter J., and Scher, Stanley H.: Status of Spin Research for Recent Airplane Designs. NASA TR R-57, 1960. (Supersedes NACA RM L57F12.)

9. Grantham, William D.: Analytical Investigation of the Spin and Recovery Characteristics of a Supersonic Trainer Airplane Having a 24° Swept Wing. NASA TM X-606, 1962.

TABLE I.- MASS AND DIMENSIONAL CHARACTERISTICS

Parameter	Configuration			
	A	B	C	D
$\bar{c}$, ft	10.27	11.83	36.17	23.755
b, ft	22.36	35.67	56.89	38.120
S, sq ft	200.00	385.33	1,542.53	695.050
W, lb	15,792	23,771	71,800	24,811
I_X, slug-ft^2	5,391	11,709	290,000	13,600
I_Y, slug-ft^2	92,249	82,654	747,000	128,000
I_Z, slug-ft^2	94,112	89,237	965,000	138,000
Maximum control deflections:				
δ_e, deg	-30.0	-30.0	-20.0	-25.0
δ_r, deg	±7.5	±6.0	±30.0	±25.0
δ_a, deg	±7.5	±15.0	±15.0	±7.5

TABLE II.- INITIAL CONDITIONS USED IN CALCULATIONS

(a) Simulated launch with rotation; $\beta = \phi_e = \psi_e = v = q = 0$

Altitude, ft	μ	α, deg	θ_e, deg	u, ft/sec	w, ft/sec	V_R, ft/sec	p, radians/sec	r, radians/sec
				Configuration A				
15,000	73	85	-5	15	172	173	0.157	1.793
30,000	123	85	-5	22	250	251	.157	1.793
45,000	273	85	-5	27	309	310	.157	1.793
60,000	487	85	-5	39	442	444	.157	1.793
				Configuration B				
15,000	36	85	-5	18	208	209	0.218	2.490
30,000	60	85	-5	24	270	271	.218	2.490
45,000	116	85	-5	33	374	376	.218	2.490
60,000	238	85	-5	47	536	538	.218	2.490
				Configuration C				
15,000	17	85	-5	13	152	153	0.131	1.494
30,000	28	85	-5	17	197	198	.131	1.494
45,000	55	85	-5	24	274	275	.131	1.494
60,000	113	85	-5	34	392	394	.131	1.494
				Configuration D				
15,000	19	85	-5	17	194	195	0.131	1.494
30,000	33	85	-5	21	244	246	.131	1.494
45,000	63	85	-5	30	340	341	.131	1.494
60,000	129	85	-5	41	468	470	.131	1.494

(b) Simulated spin entry; $\beta = \phi_e = \psi_e = v = p = r = 0$

Altitude, ft	μ	α, deg	θ_e, deg	u, ft/sec	w, ft/sec	V_R, ft/sec	q, radians/sec
				Configuration A			
15,000	73	25	25	208	97	230	0.3
30,000	123	25	25	269	126	297	0.3
45,000	273	25	25	374	174	412	0.3
60,000	487	25	25	535	249	590	0.3
				Configuration B			
15,000	36	10	10	431	76	438	0
30,000	60	10	10	587	104	596	0
45,000	116	10	10	776	137	788	0
60,000	238	10	10	1,110	196	1,127	0
				Configuration C			
15,000	17	20	0	263	96	280	0
30,000	28	20	0	341	125	364	0
45,000	55	20	0	474	172	504	0
60,000	113	20	0	678	247	722	0
				Configuration D			
15,000	19	18	18	243	79	255	0
30,000	33	18	18	315	102	331	0
45,000	63	18	18	437	141	459	0
60,000	129	18	18	625	203	657	0

TABLE III.- SOME PERTINENT RESULTS OBTAINED WHEN CONFIGURATIONS WERE LAUNCHED INTO A NEAR-SPIN CONDITION

[All values taken after approximately 10 turns except where noted]

Initial altitude, h_0, ft	Initial μ	α, deg	β, deg	r, radians/sec	V, ft/sec	$\Omega b/2V_R$	Turns for recovery	Figure
Configuration A								
15,000	73	84 to 89	1 to -8	2.8	181	0.17	No recovery	9(a)
30,000	123	84 to 90	3 to -8	2.9	230	.14	--------	None
45,000	273	85 to 88	1 to -6	3.0	302	.11	No recovery	None
60,000	487	85 to 88	0 to -4	3.1	418	.09	No recovery	(9b)
Configuration B								
15,000	36	70 to 80	4 to -7	2.1	202	0.20	7	10(a)
30,000	60	73 to 81	3 to -6	2.3	254	.17	7	None
45,000	116	74 to 82	4 to -7	2.6	329	.14	>9	None
60,000	238	77 to 82	3 to -5	2.8	449	.12	>9	10(b)
Configuration C								
15,000	17	70 to 90	5 to -12	1.6	202	0.22	No recovery	11(a)
30,000	28	70 to 88	5 to -10	1.7	243	.17	--------	None
45,000	55	75 to 85	5 to -10	1.7	319	.15	--------	None
60,000	113	75 to 85	5 to -10	1.8	431	.12	No recovery	11(b)
Configuration D								
15,000	19	74	-2	1.2	172	0.13	$2\frac{1}{2}$	12(a)
30,000	33	75	-2	1.3	219	.12	--------	None
45,000	63	75 to 78	-2	1.5	277	.10	4	None
60,000	129	76 to 80	-1 to -2	1.6	372	.08	5	12(b)

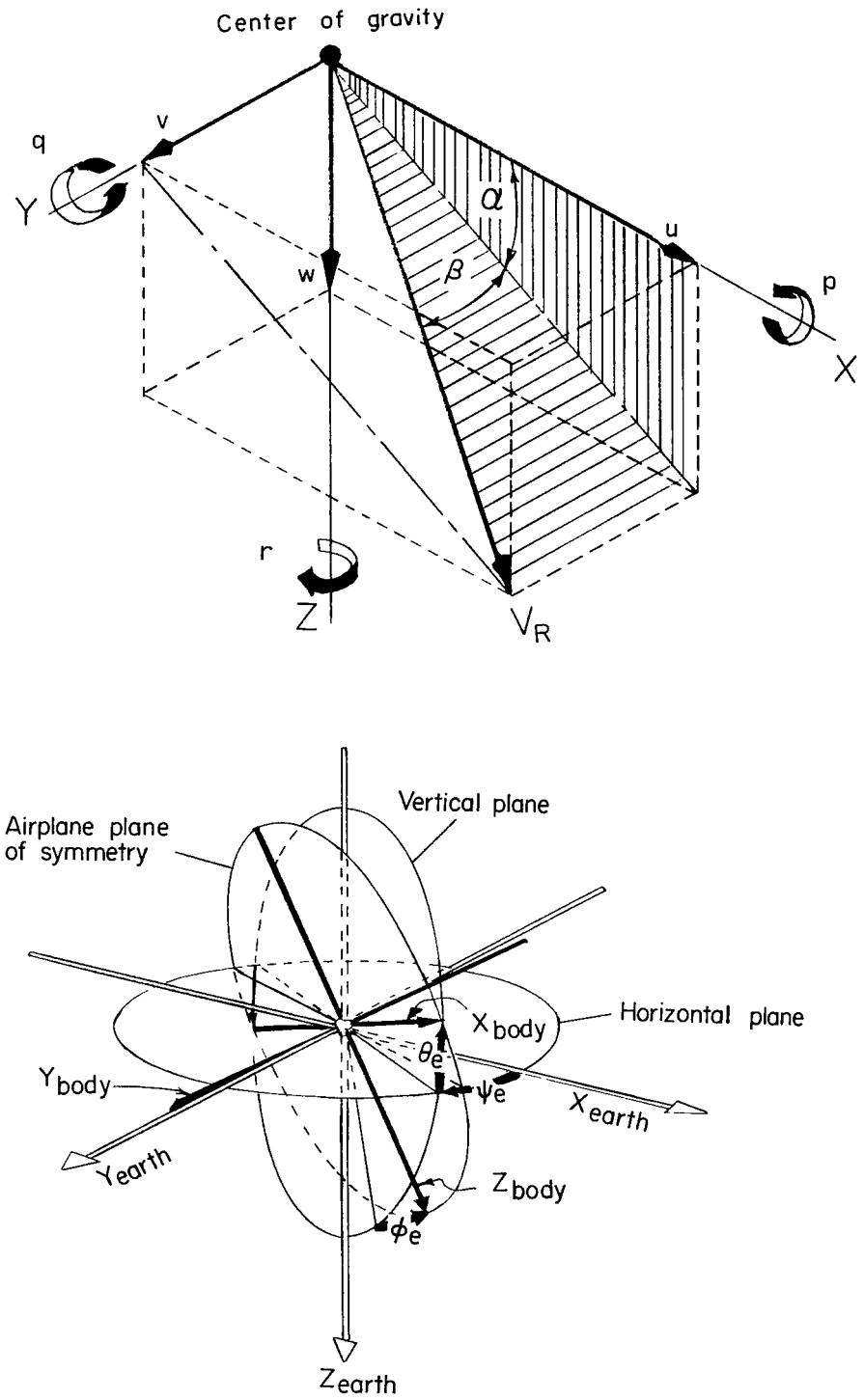

Figure 1.- Body system of axes and related angles. Arrows indicate positive directions.

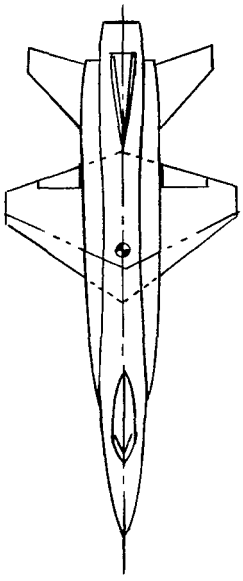

Configuration A

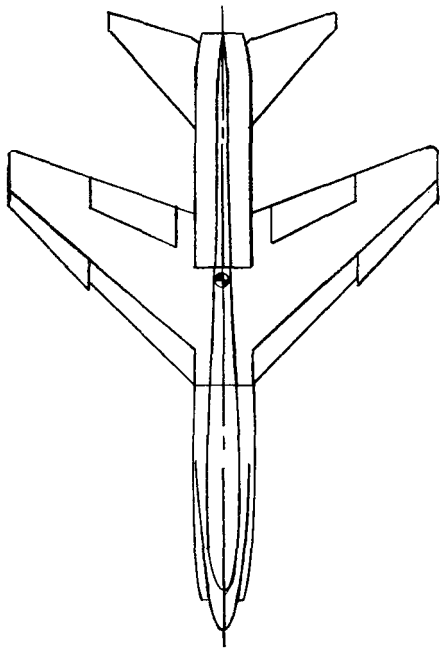

Configuration B

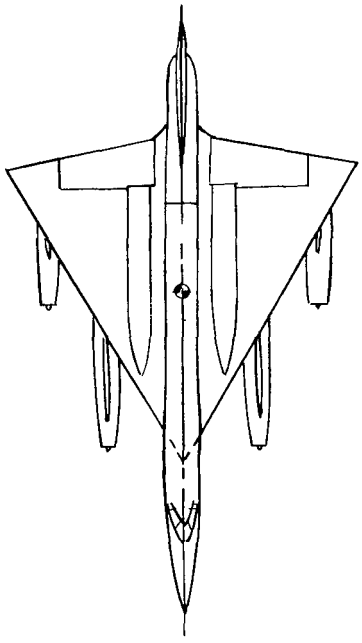

Configuration C

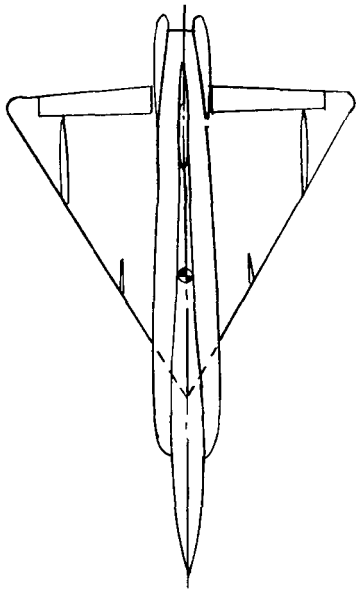

Configuration D

Figure 2.- Planview of four configurations studied.

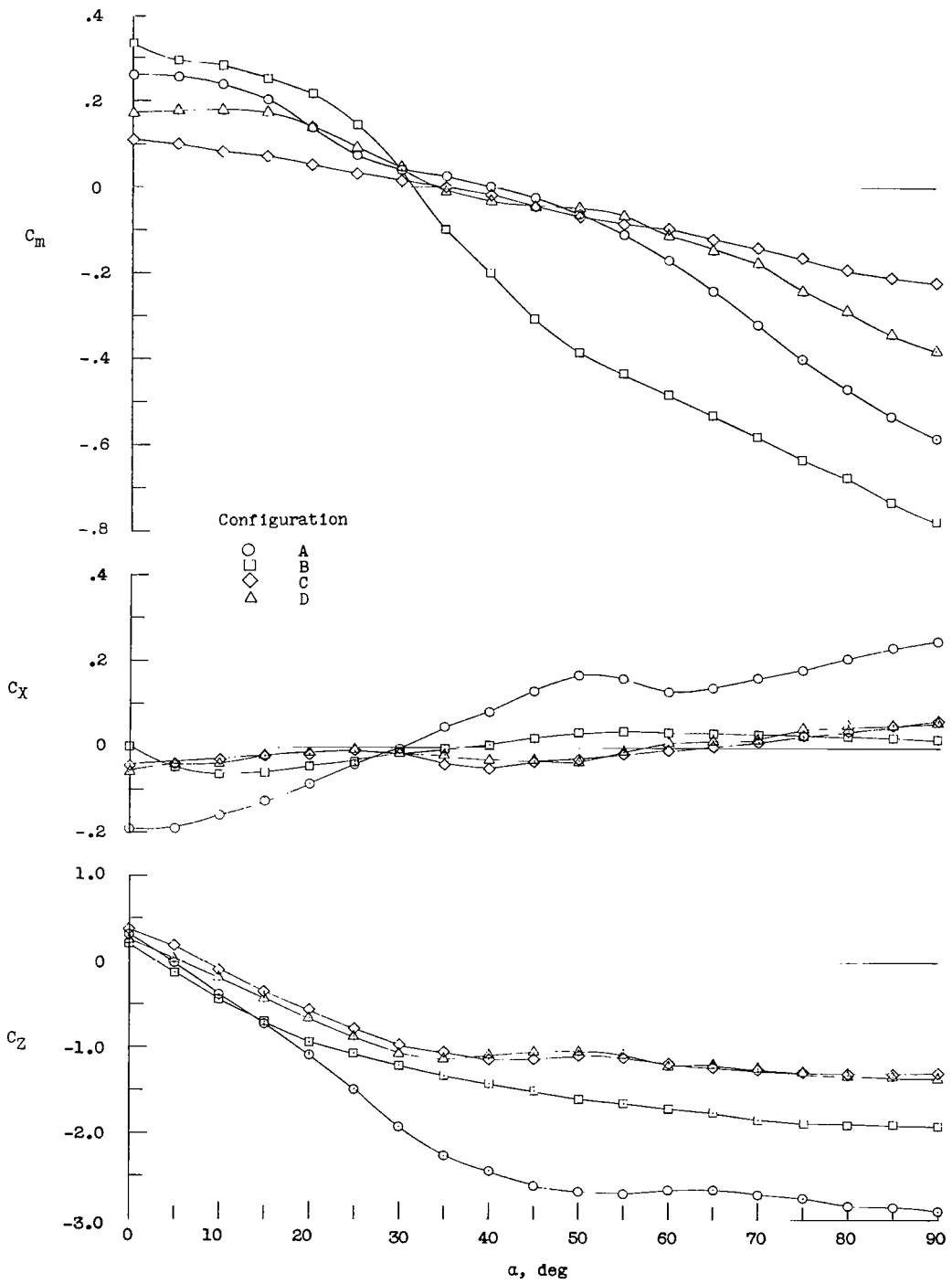

Figure 3.- Variations of pitching-moment, longitudinal-force, and vertical-force coefficients with angle of attack.

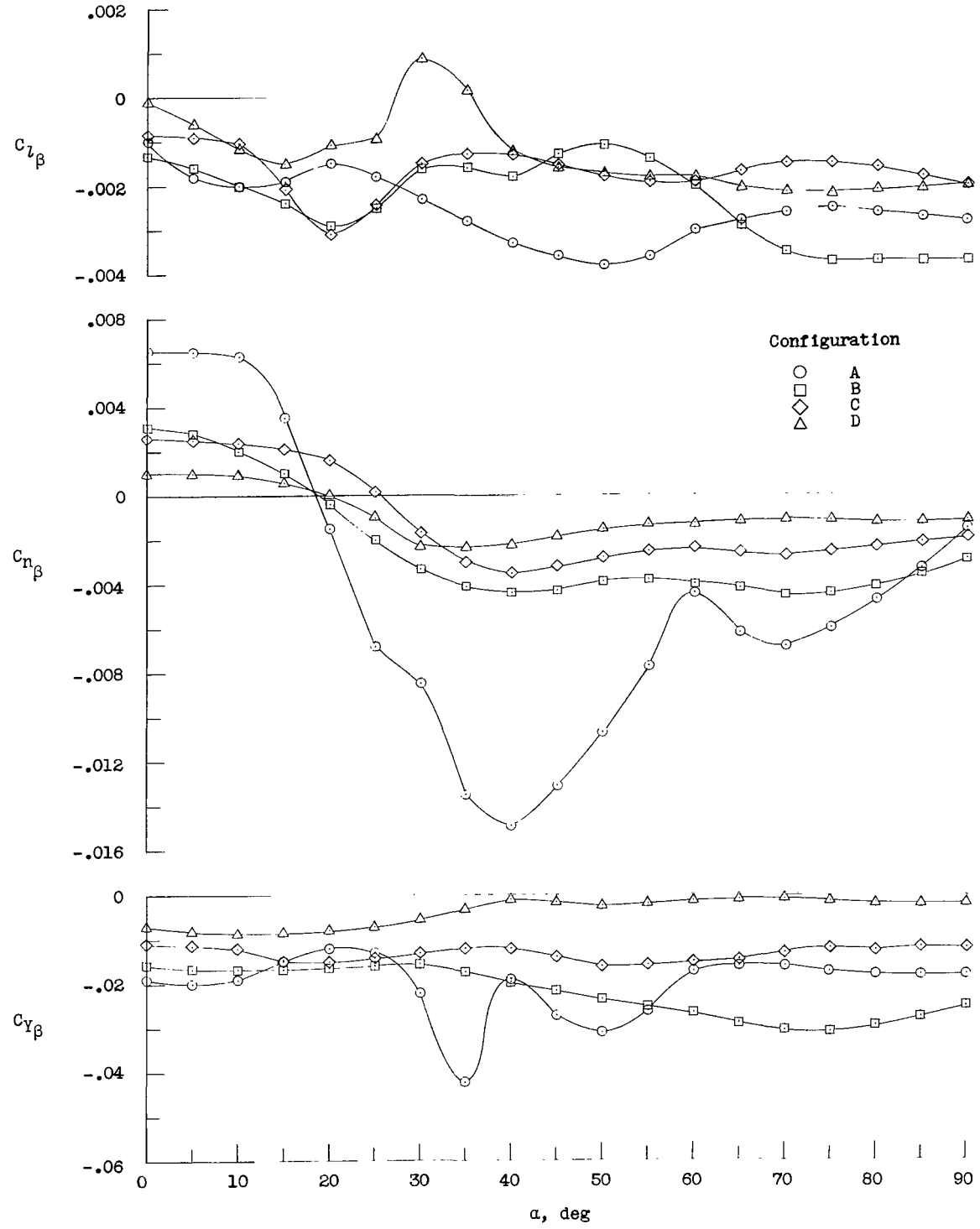

Figure 4.- Variations of sideslip derivatives with angle of attack.

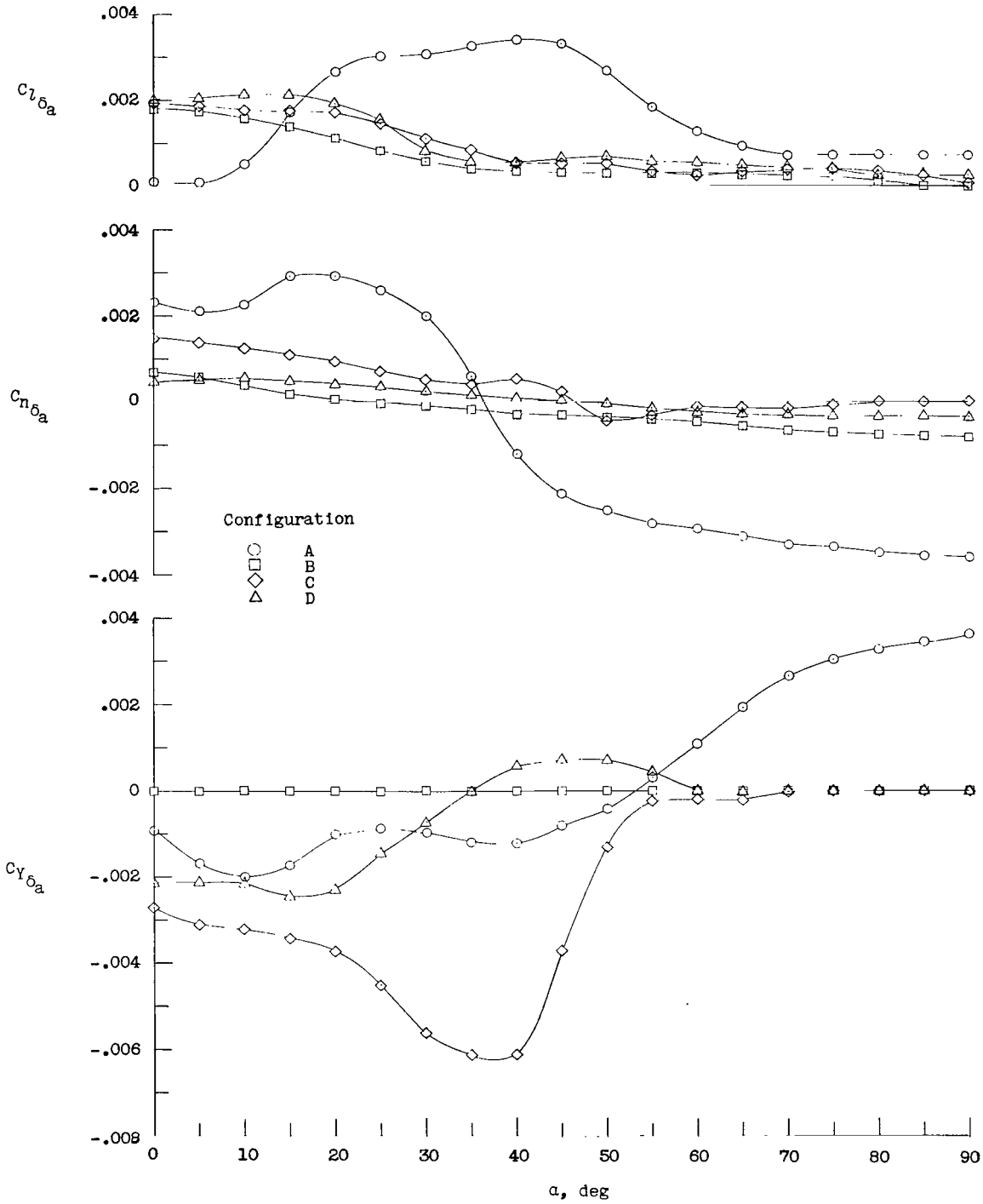

Figure 5.- Variation in increments in lateral-force and moment coefficients with angle of attack due to deflecting the ailerons.

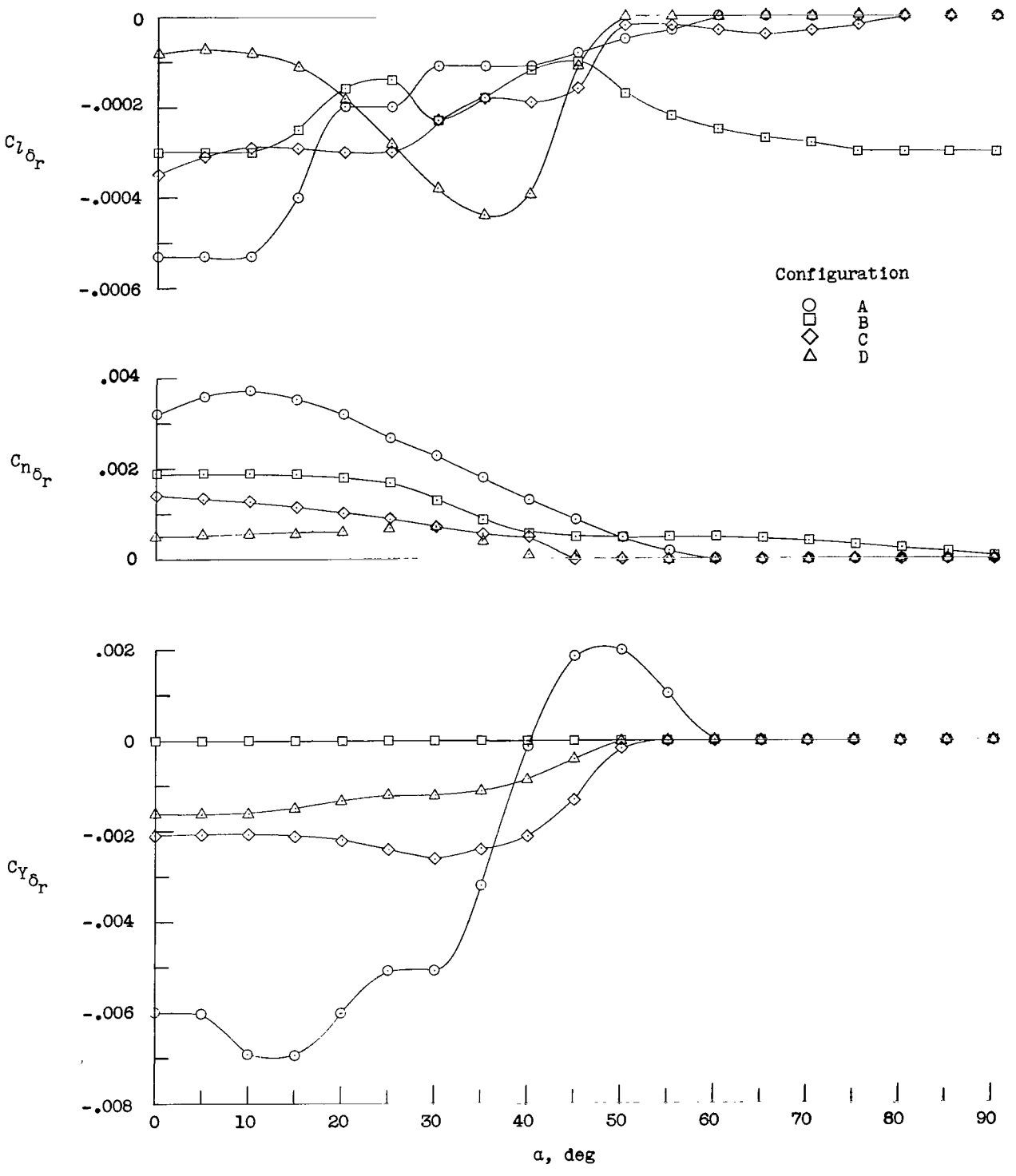

Figure 6.- Variation in increments in lateral-force and moment ccefficients with angle of attack resulting from a rudder deflection.

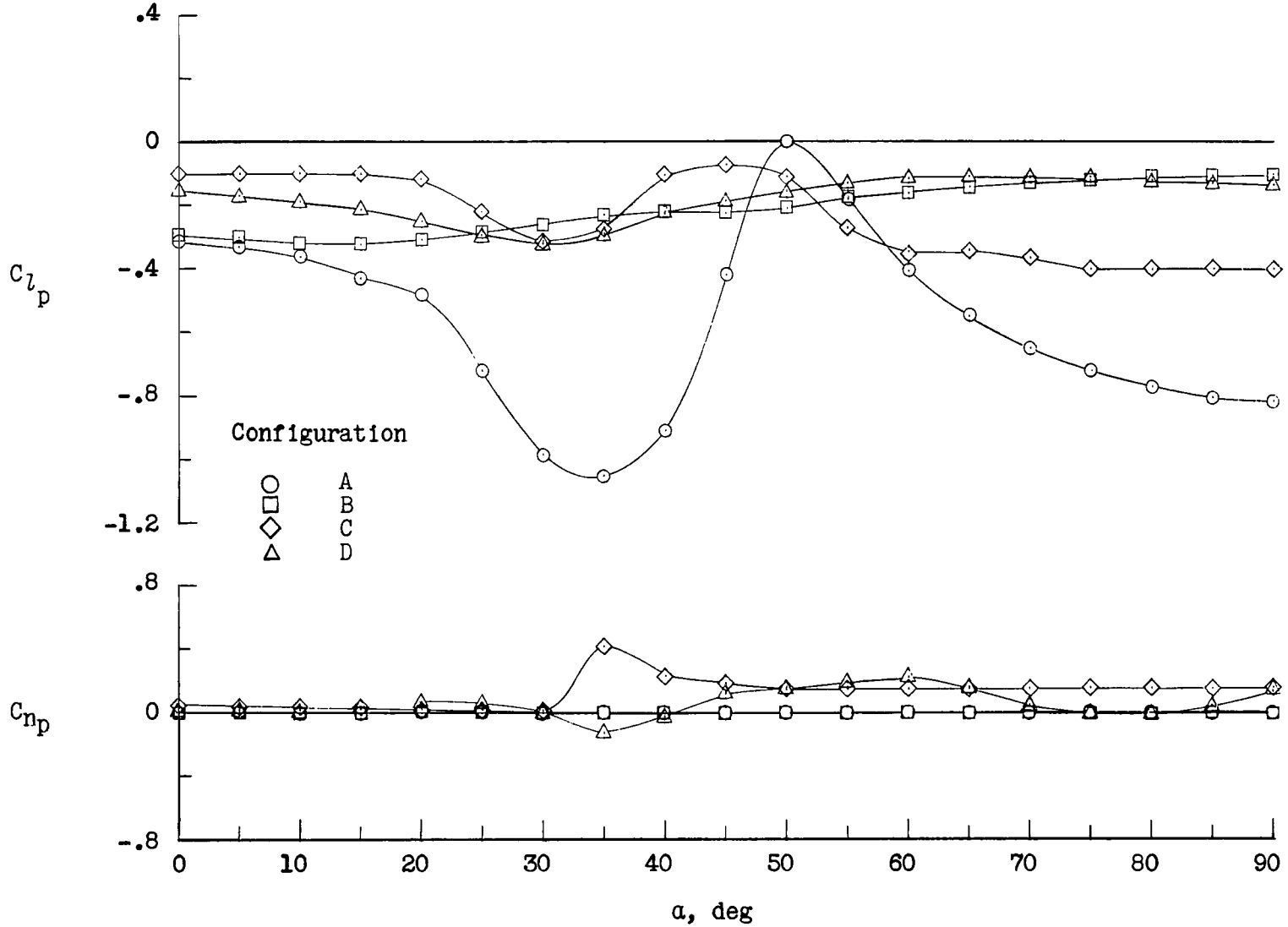

Figure 7.- Variation of out-of-phase rolling derivatives with angle of attack.

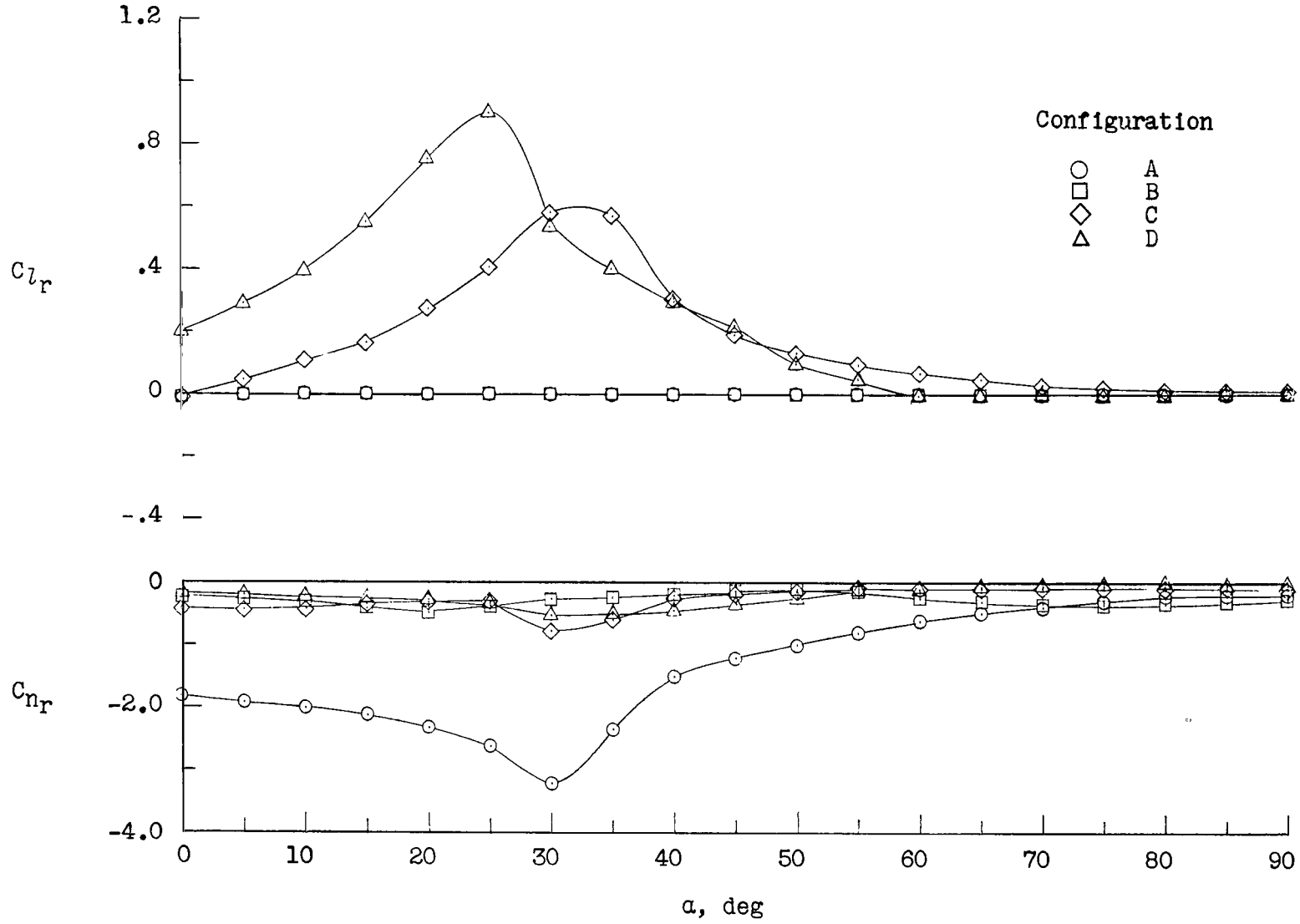

Figure 8.- Variation of out-of-phase yawing derivatives with angle of attack.

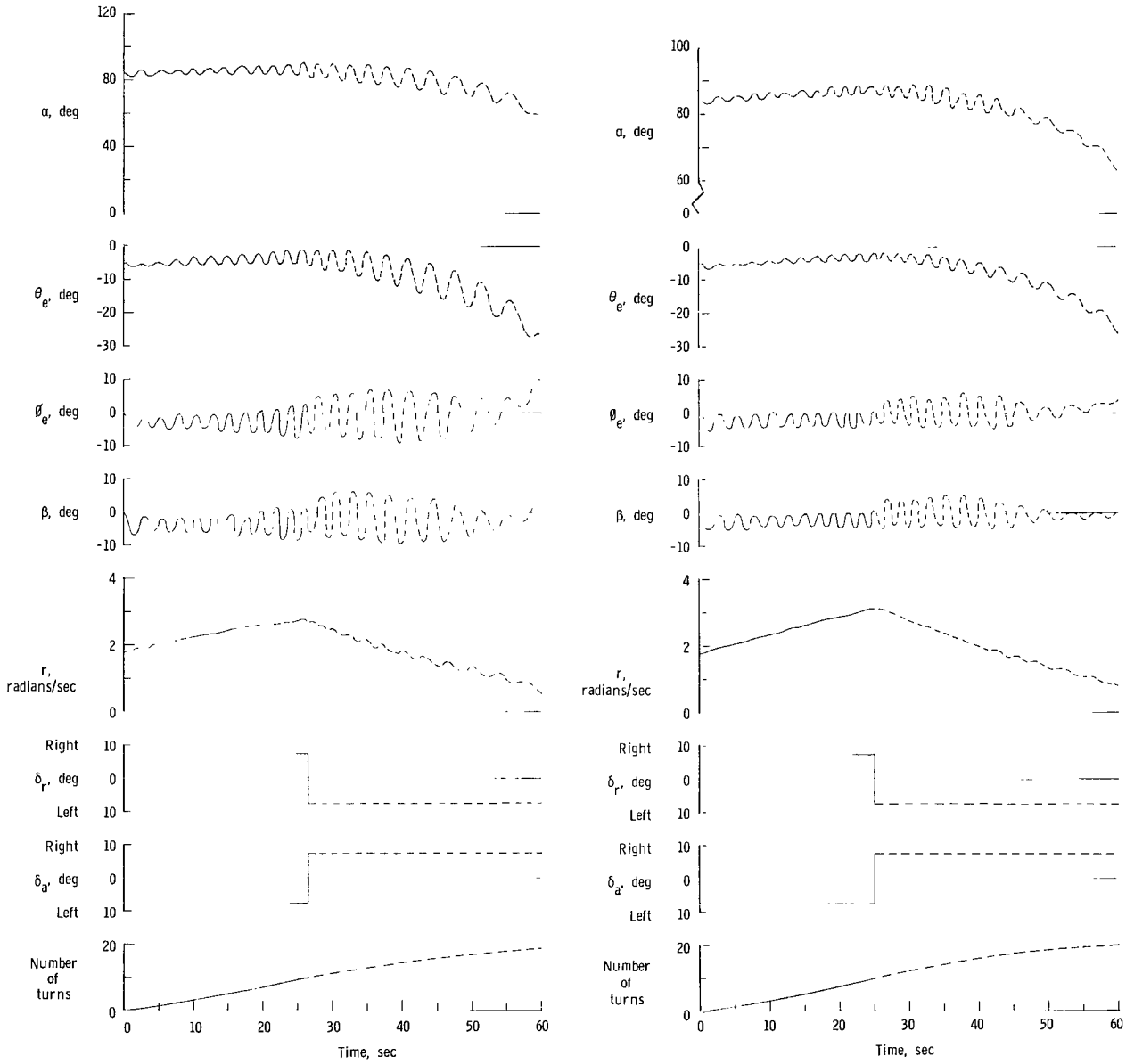

(a) h_0 = 15,000 ft. (b) h_0 = 60,000 ft.

Figure 9.- Calculation simulating launching with rotary motion. Configuration A; $\delta_e = -30^\circ$.

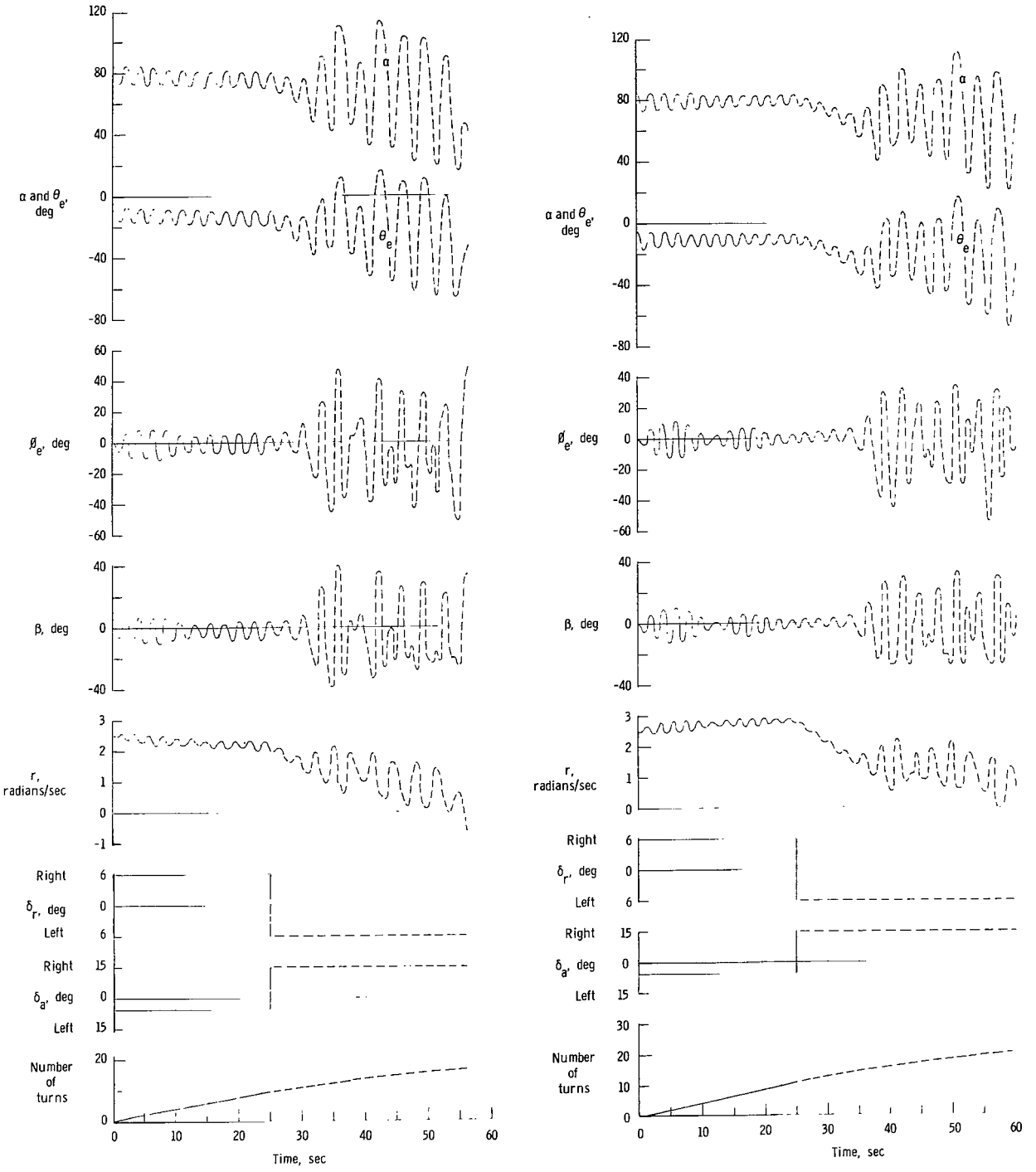

(a) h_0 = 15,000 ft.

(b) h_0 = 60,000 ft.

Figure 10.- Calculation simulating launching with rotary motion. Configuration B; $\delta_e = -30^\circ$.

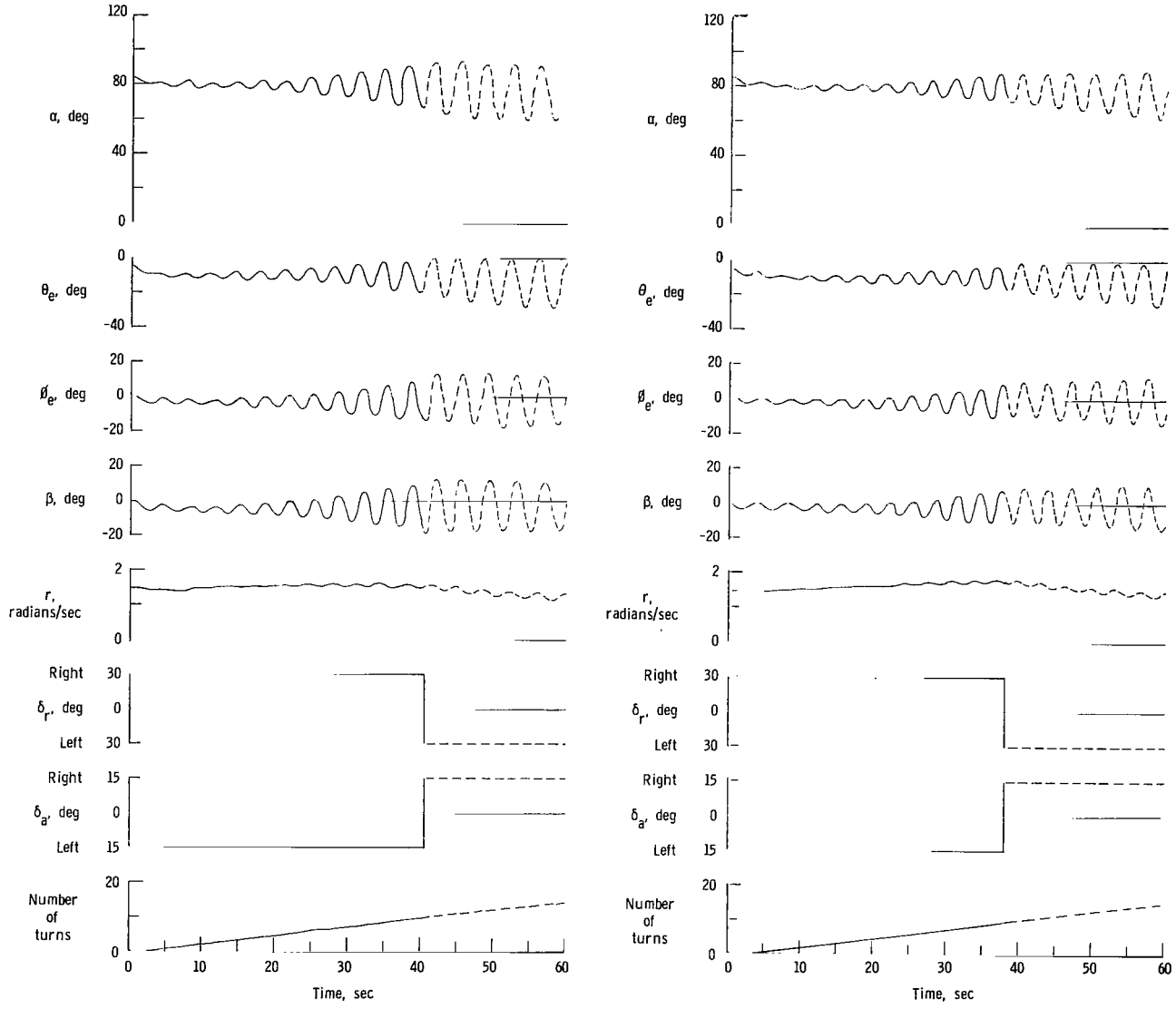

(a) h_0 = 15,000 ft.

(b) h_0 = 60,000 ft.

Figure 11.- Calculation simulating launching with rotary motion. Configuration C; $\delta_e = -20^\circ$.

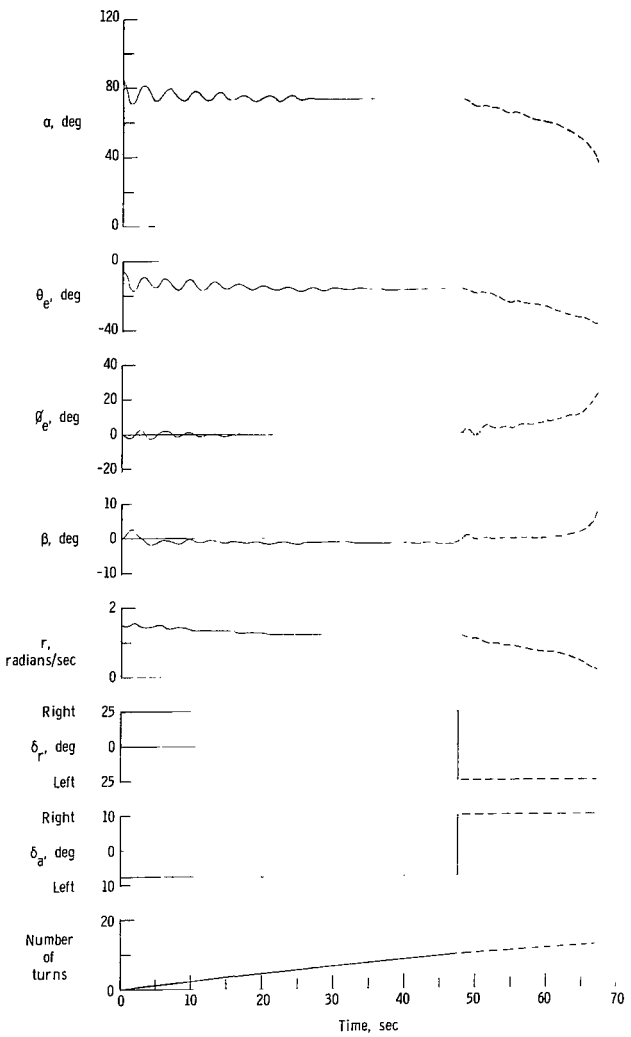

(a) h_0 = 15,000 ft.

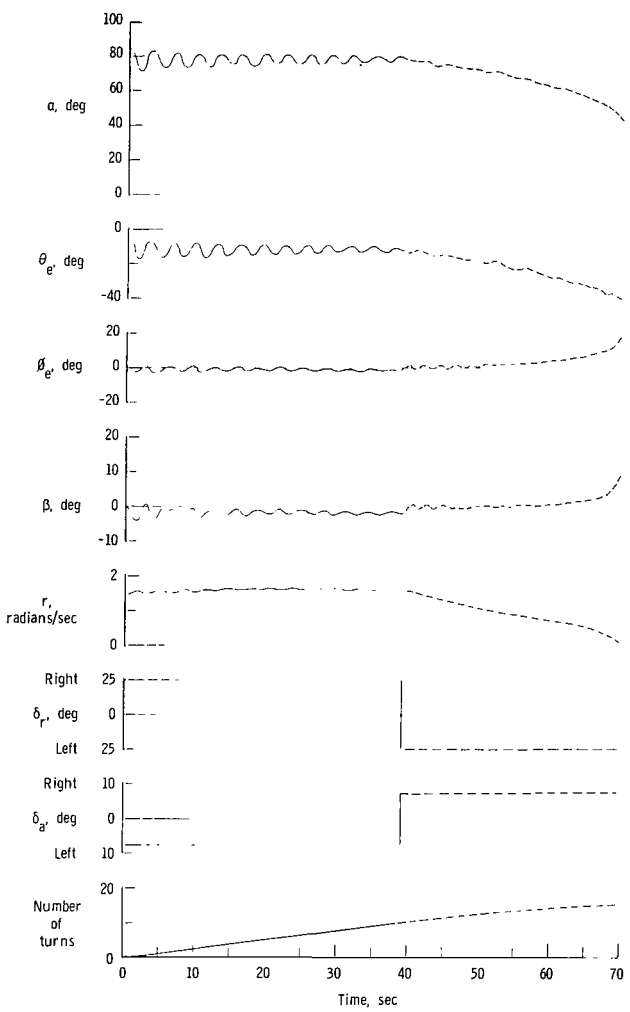

(b) h_0 = 60,000 ft.

Figure 12.- Calculation simulating launching with rotary motion. Configuration D; $\delta_e = -25^\circ$.

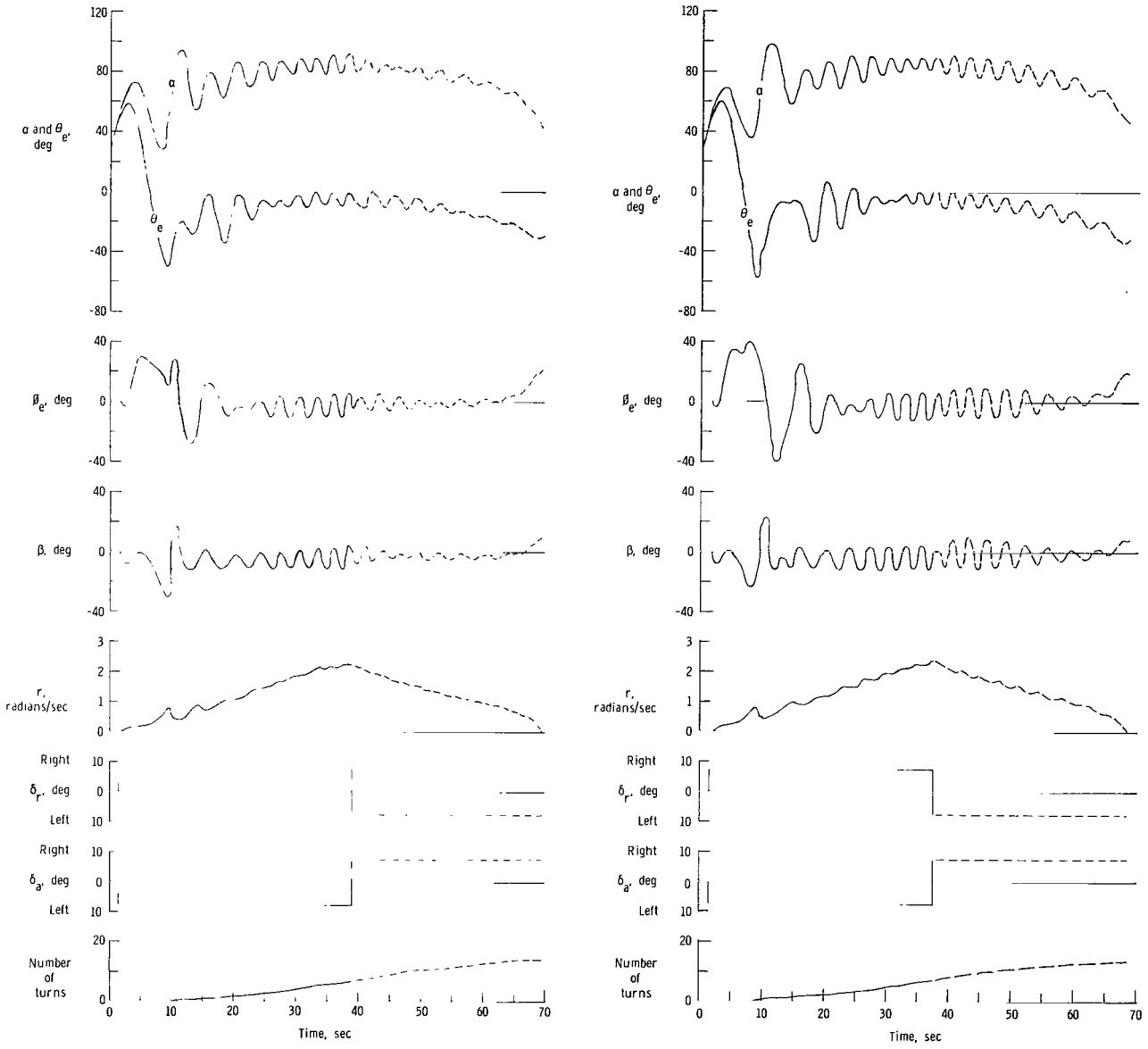

(a) h_0 = 15,000 ft. (b) h_0 = 30,000 ft.

Figure 13.- Calculated spin entry attempt. Configuration A; $\delta_e = -30^\circ$.

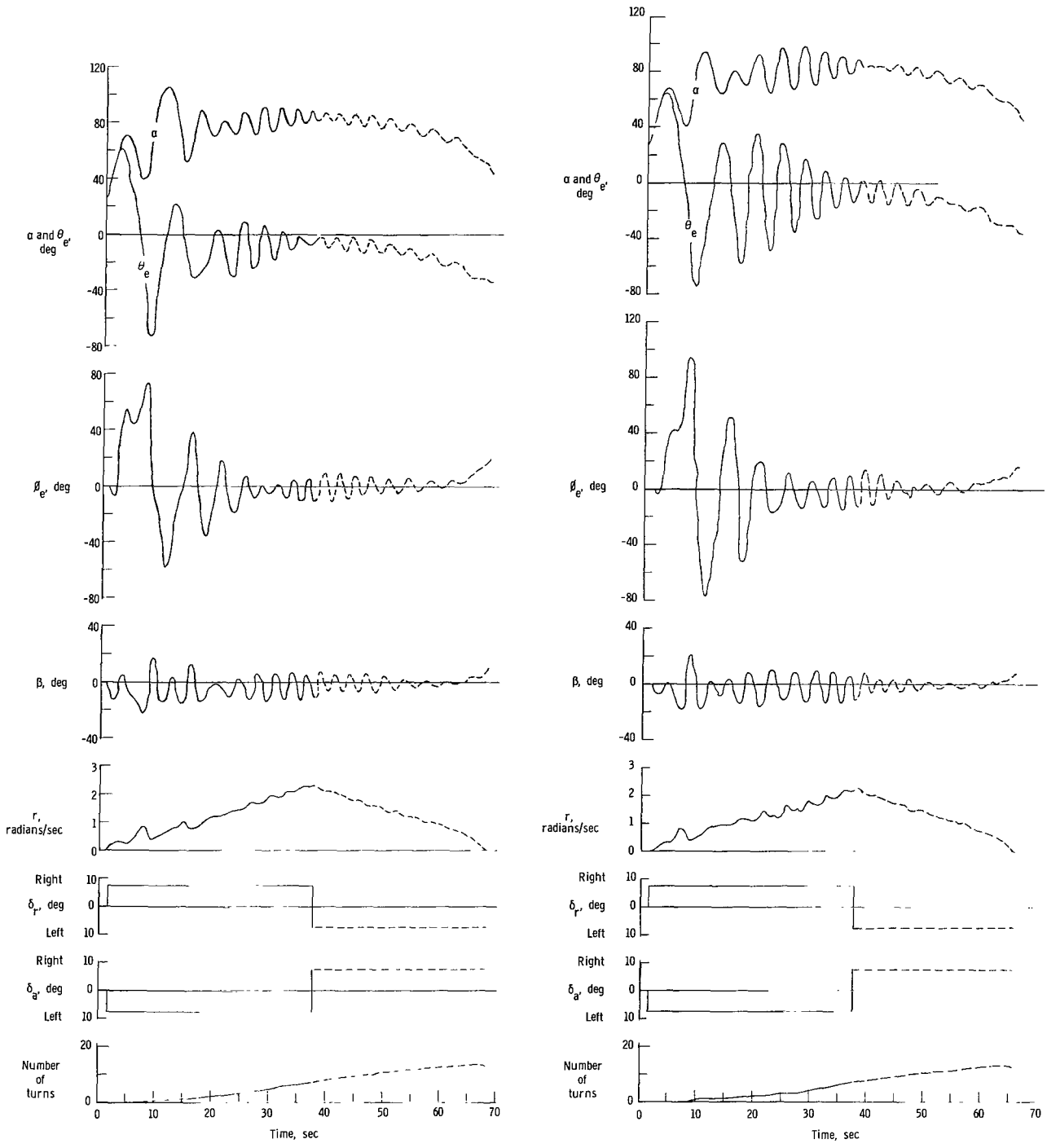

(c) h_0 = 45,000 ft.

(d) h_0 = 60,000 ft.

Figure 13.- Concluded.

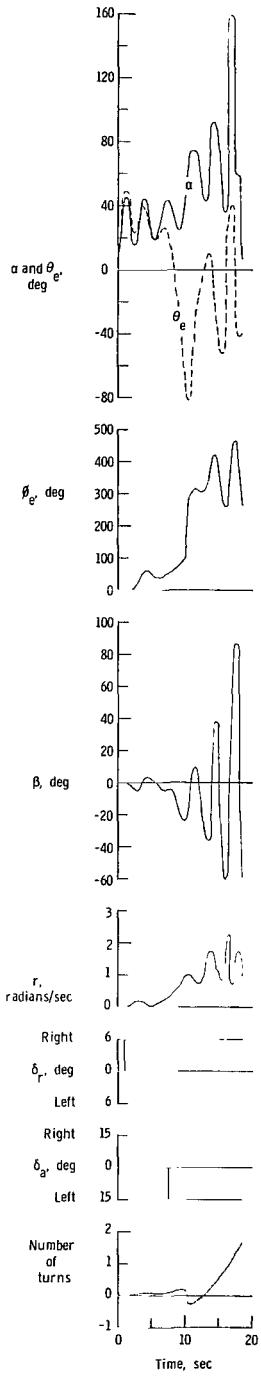

(a) h_0 = 15,000 ft.

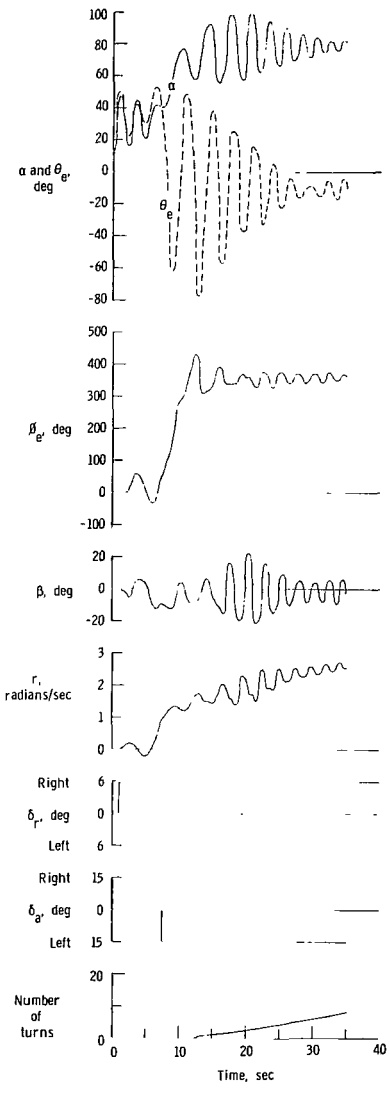

(b) h_0 = 30,000 ft.

Figure 14.- Calculated spin entry attempt. Configuration B; $\delta_e = -30^\circ$.

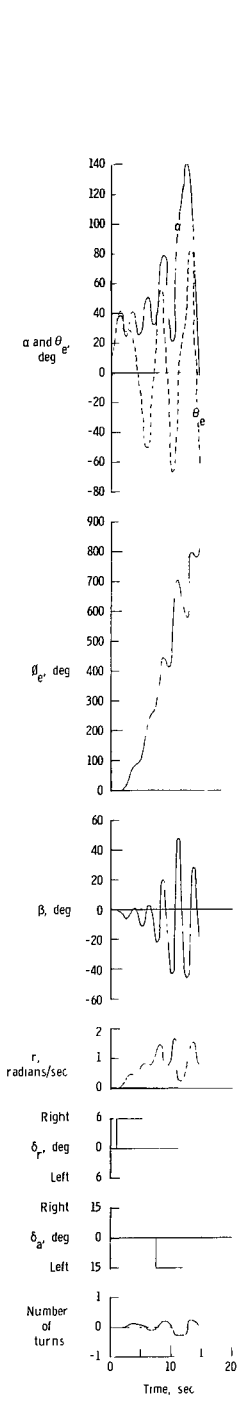

(c) h_0 = 45,000 ft.

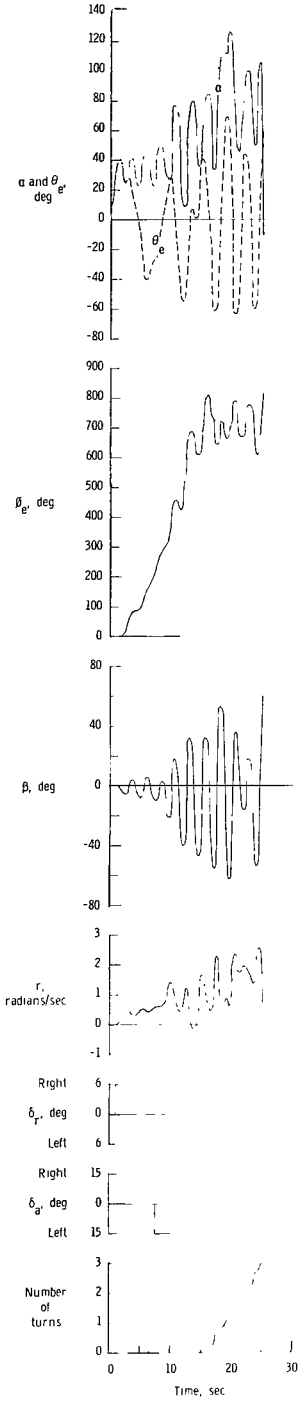

(d) h_0 = 60,000 ft.

Figure 14.- Concluded.

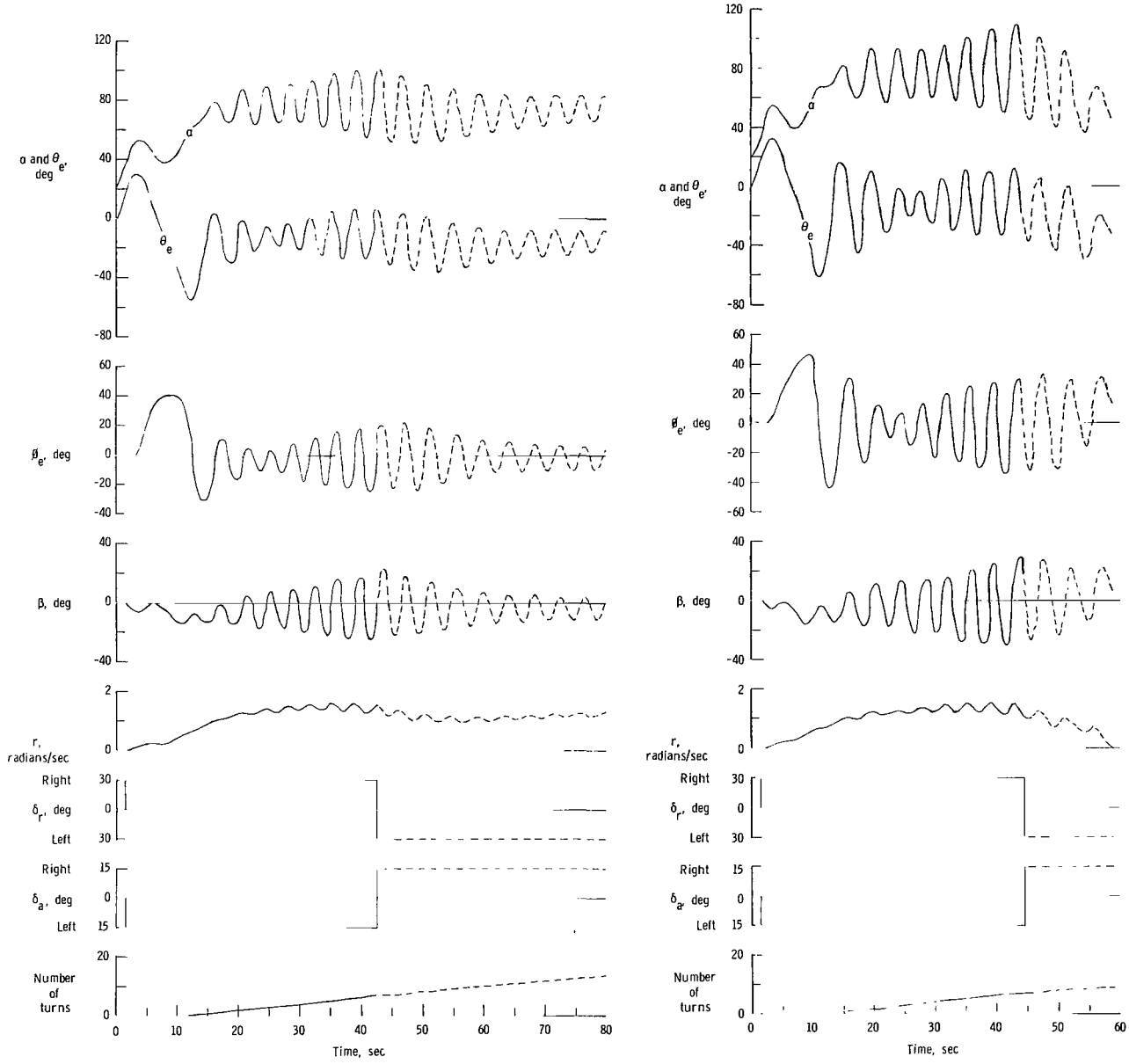

(a) h_0 = 15,000 ft. (b) h_0 = 30,000 ft.

Figure 15.- Calculated spin entry attempt. Configuration C; δ_e = -20°.

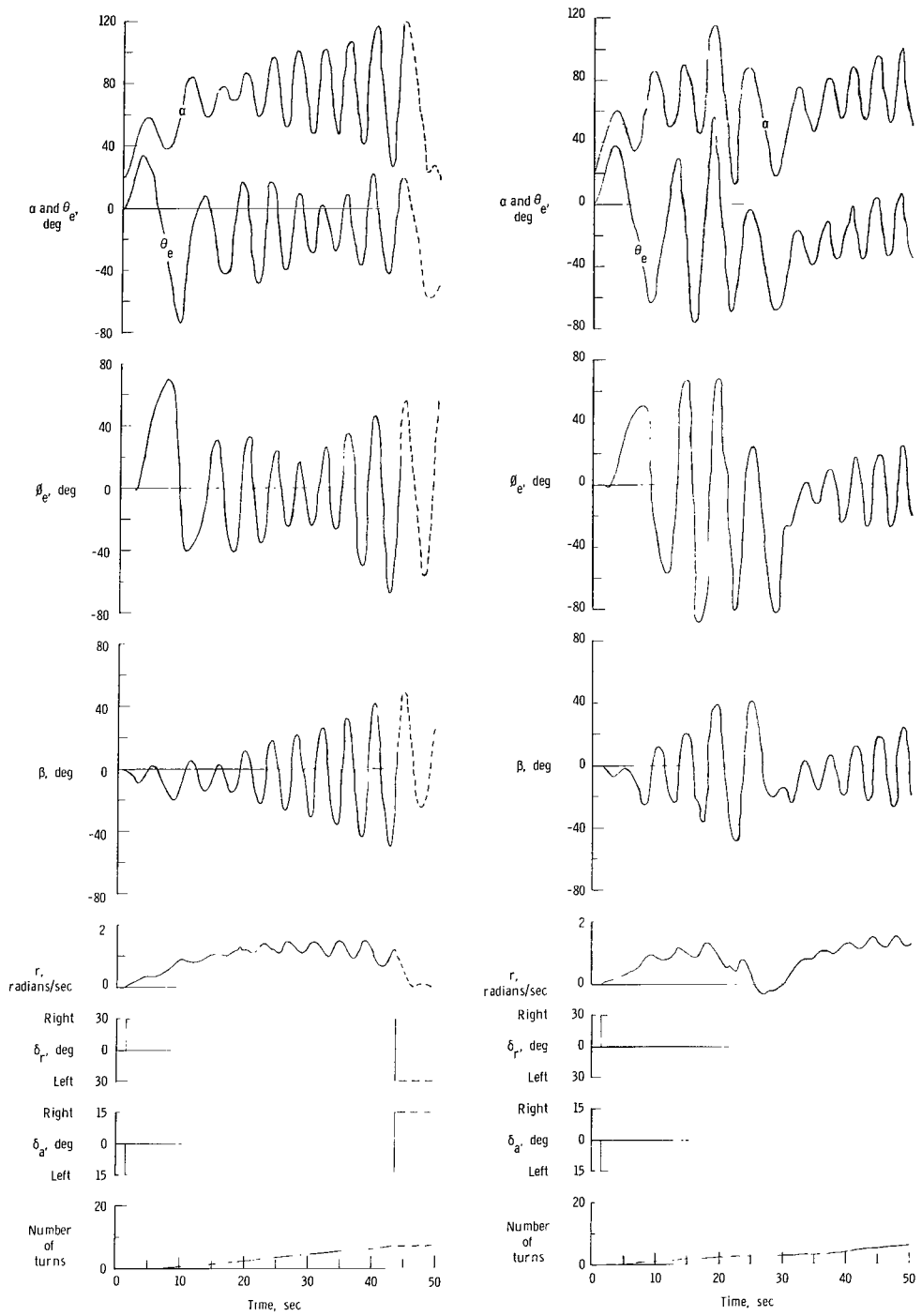

(c) h_0 = 45,000 ft.

(d) h_0 = 60,000 ft.

Figure 15.- Concluded.

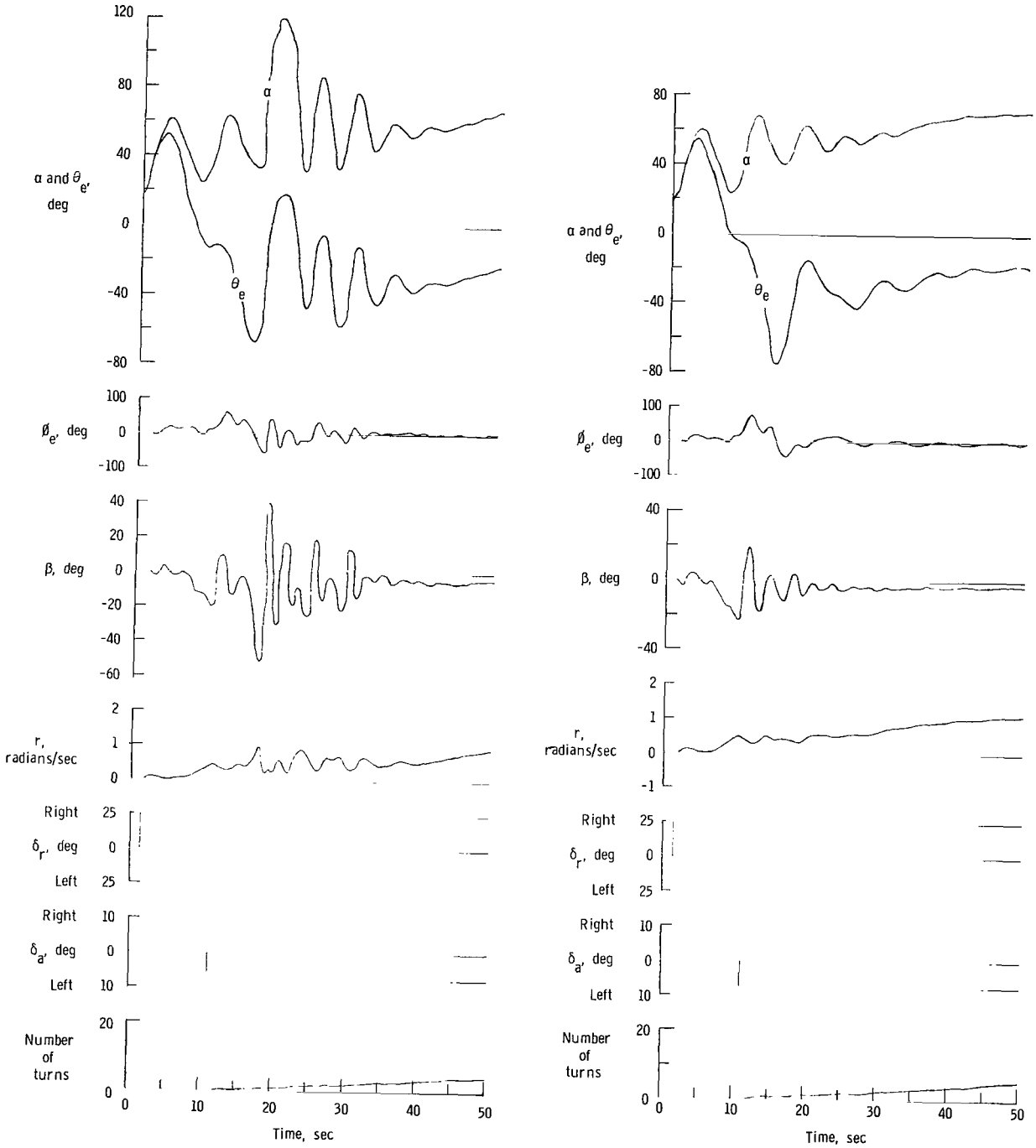

(a) h_0 = 15,000 ft.

(b) h_0 = 30,000 ft.

Figure 16.- Calculated spin entry attempt. Configuration D; δ_e = -25°.

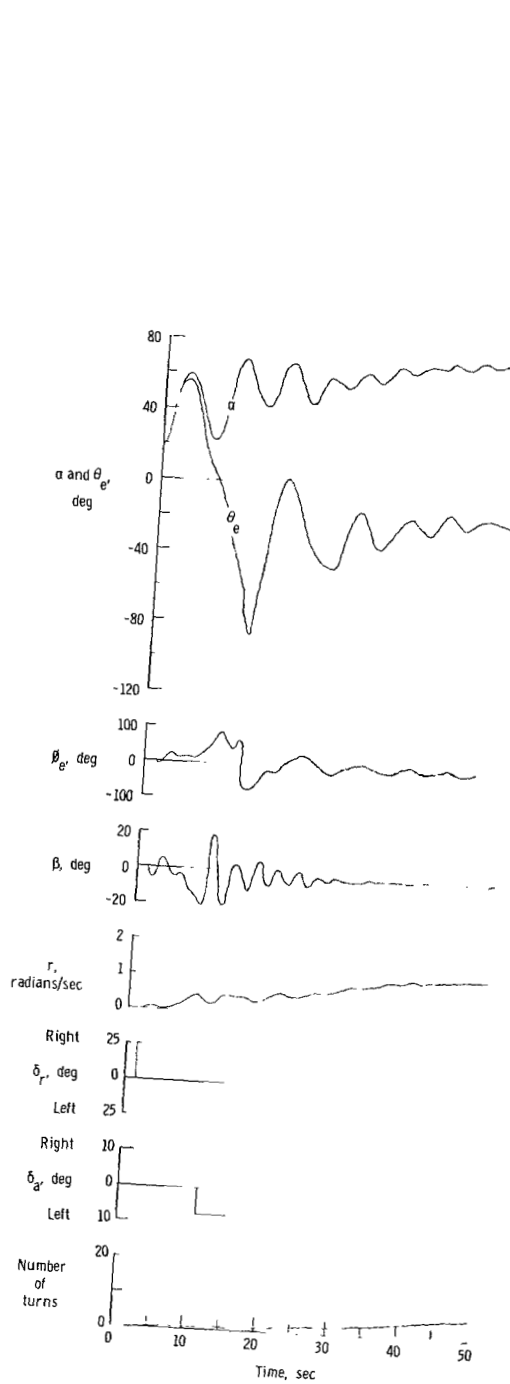

(c) h_0 = 45,000 ft.

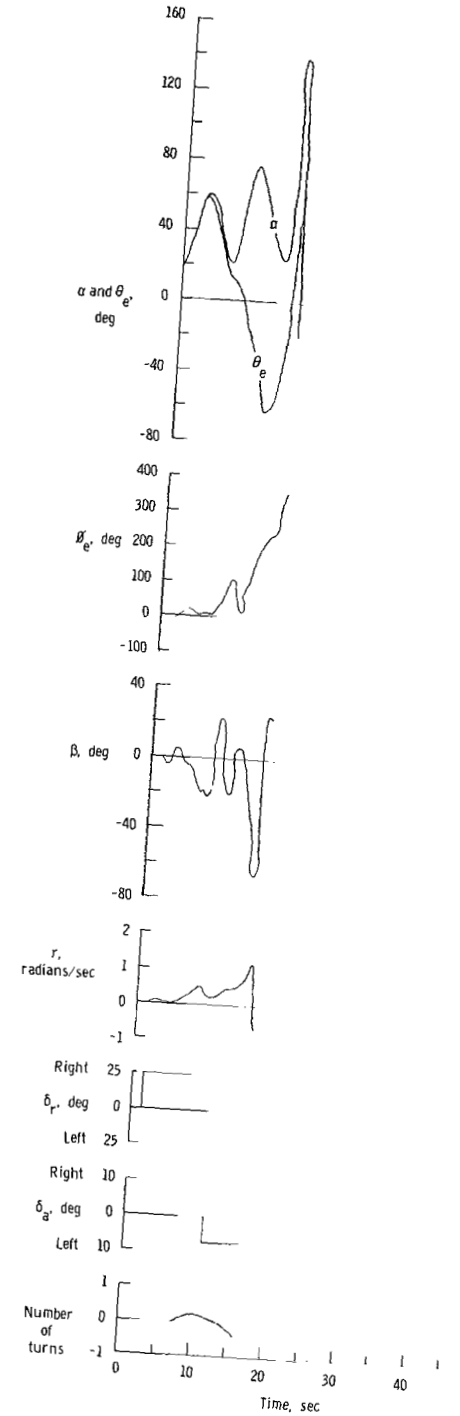

(d) h_0 = 60,000 ft.

Figure 16.- Concluded.

NASA-Langley, 1965 L-3915

2/7/05

"The aeronautical and space activities of the United States shall be conducted so as to contribute . . . to the expansion of human knowledge of phenomena in the atmosphere and space. The Administration shall provide for the widest practicable and appropriate dissemination of information concerning its activities and the results thereof."

—NATIONAL AERONAUTICS AND SPACE ACT OF 1958

NASA SCIENTIFIC AND TECHNICAL PUBLICATIONS

TECHNICAL REPORTS: Scientific and technical information considered important, complete, and a lasting contribution to existing knowledge.

TECHNICAL NOTES: Information less broad in scope but nevertheless of importance as a contribution to existing knowledge.

TECHNICAL MEMORANDUMS: Information receiving limited distribution because of preliminary data, security classification, or other reasons.

CONTRACTOR REPORTS: Technical information generated in connection with a NASA contract or grant and released under NASA auspices.

TECHNICAL TRANSLATIONS: Information published in a foreign language considered to merit NASA distribution in English.

TECHNICAL REPRINTS: Information derived from NASA activities and initially published in the form of journal articles.

SPECIAL PUBLICATIONS: Information derived from or of value to NASA activities but not necessarily reporting the results of individual NASA-programmed scientific efforts. Publications include conference proceedings, monographs, data compilations, handbooks, sourcebooks, and special bibliographies.

Details on the availability of these publications may be obtained from:

SCIENTIFIC AND TECHNICAL INFORMATION DIVISION

NATIONAL AERONAUTICS AND SPACE ADMINISTRATION

Washington, D.C. 20546